nature COMMUNICATIONS

PERSPECTIVE

https://doi.org/10.1038/s41467-019-13638-9 OPEN

CO_2 hydrogenation to high-value products via heterogeneous catalysis

Run-Ping Ye[1,2,3,11], Jie Ding[1,4,11], Weibo Gong[1,11], Morris D. Argyle[5], Qin Zhong[4], Yujun Wang[6], Christopher K. Russell[1,7], Zhenghe Xu[8], Armistead G. Russell[9], Qiaohong Li[2], Maohong Fan[1,9,10*] & Yuan-Gen Yao[2*]

Recently, carbon dioxide capture and conversion, along with hydrogen from renewable resources, provide an alternative approach to synthesis of useful fuels and chemicals. People are increasingly interested in developing innovative carbon dioxide hydrogenation catalysts, and the pace of progress in this area is accelerating. Accordingly, this perspective presents current state of the art and outlook in synthesis of light olefins, dimethyl ether, liquid fuels, and alcohols through two leading hydrogenation mechanisms: methanol reaction and Fischer-Tropsch based carbon dioxide hydrogenation. The future research directions for developing new heterogeneous catalysts with transformational technologies, including 3D printing and artificial intelligence, are provided.

Capturing carbon dioxide (CO_2) has emerged as an important method of mitigating its impact on environment[1–5]. However, this introduces the challenge of utilizing a large volume of captured CO_2, which previously has not had any industrially viable uses at such a large scale. Realizing that, historically, fossil resources were produced via natural carbon-hydrogenation during photosynthesis, synthetic CO_2 hydrogenation is likely the best way to regenerate combusted hydrocarbons.

While CO_2 hydrogenation is challenging due to the thermal stability of CO_2, making reaction conversions low, considerable progress has been made towards converting CO_2 to single carbon (C_1) products (e.g., formic acid, carbon monoxide (CO), methane, and methanol) through direct hydrogen reduction or hydrothermal-chemical reduction in water[6–11]. Thermocatalytic hydrogenation of CO_2 to methane can be achieved easily at atmospheric pressure and high gas hourly space velocity (GHSV), and has been shown to achieve CO_2 conversion and CH_4 selectivity close to theoretical equilibrium values[12]. Hydrogenation to CO can be performed via the reverse water gas shift (RWGS) reaction. CO_2-to-methanol (CTM) (CH_3OH and MeOH) has already been industrialized in Reykjavik, Iceland using heterogeneous catalysis and geothermal energy[13].

[1] Departments of Chemical and Petroleum Engineering, University of Wyoming, Laramie, WY 82071, USA. [2] Key Laboratory of Coal to Ethylene Glycol and Its Related Technology, Fujian Institute of Research on the Structure of Matter, Chinese Academy of Sciences, Fuzhou, Fujian 350002, China. [3] University of Chinese Academy of Sciences, Beijing 100049, China. [4] School of Chemical Engineering, Nanjing University of Science and Technology, Nanjing, Jiangsu 210094, P.R. China. [5] Department of Chemical Engineering, Brigham Young University, 330 EB, Provo, UT 84602, USA. [6] State Key Laboratory of Chemical Engineering, Department of Chemical Engineering, Tsinghua University, Beijing 100084, P.R. China. [7] Departments of Civil and Environmental Engineering, Stanford University, Stanford 94305 CA, USA. [8] Department of Materials Science and Engineering, Southern University of Science and Technology, Shenzhen 518055, China. [9] School of Civil and Environmental Engineering, Georgia Institute of Technology, Mason Building, 790 Atlantic Drive, Atlanta, GA 30332, USA. [10] School of Energy Resources, University of Wyoming, Laramie, WY 82071, USA. [11] These authors contributed equally: Run-Ping Ye, Jie Ding, Weibo Gong. *email: mfan@uwyo.edu; yyg@fjirsm.ac.cn

In addition, catalysis for CO_2 hydrogenation to C_1 products has been widely studied with considerable progress[14]. Recently, significant progress has been achieved in heterogeneous catalytic hydrogenation of CO_2 to various high-value and easily marketable fuels and chemicals containing two or more carbons (C_{2+} species), including dimethyl ether (DME)[15], olefins[16], liquid fuels[17], and higher alcohols[18]. Compared to C_1 products, C_{2+} product synthesis is more challenging due to the extreme inertness of CO_2 and the high C–C coupling barrier, as well as many competing reactions leading to the formation of C_1 products. However, C_{2+} hydrocarbons and oxygenates possess higher economic values and energy densities than C_1 compounds. Therefore, this perspective mainly focuses on heterogeneous catalysis for CO_2 hydrogenation to high-value C_{2+} products.

Many reviews of heterogeneous catalytic hydrogenation of CO_2 have been published, organized according to using several approaches, including thermal, electrochemical, and photochemical hydrogenation[19]; homogeneous and heterogeneous catalysts[20]; and by their respective product distributions or catalysts employed[14,21–24]. Some are limited to C_1 products (e.g., methane or methanol)[14,25]. However, perspectives on heterogeneous catalytic CO_2 hydrogenation to C_{2+} products are needed to guide scientists working in this area. Thus, this work is designed to help fill this gap and is organized to emphasize reaction mechanisms for producing C_{2+} materials.

The hydrogenation of CO_2 to C_{2+} products mainly occurs via a methanol-mediated route or a CO_2 modified Fischer–Tropsch mechanism[17,26]. There are a variety of questions that need to be answered for each of these reaction mechanisms: what kinds of catalysts are beneficial for each route? How do the catalysts regulate product selectivity? What can be done to further enhance catalytic performance? What is the central challenge with catalysts for CO_2 hydrogenation to C_{2+} products? To answer these questions, the catalysts for CO_2 hydrogenation to C_{2+} species will be discussed based on the methanol-mediated route and the CO_2 modified Fischer–Tropsch route. Some experimental guidelines are provided to improve CO_2 conversion and to reduce C_1 byproducts. In addition, an outlook of transformational technologies for developing new catalysts is given in this work. Artificial intelligence (AI) is expected to guide the design and discovery of catalysis[27,28], while 3D printing technologies are anticipated to be used to manufacture them on a large scale[29].

Methanol reaction based CO_2 hydrogenation

Methanol (CH_3OH) reaction based CO_2 hydrogenation can be realized by coupling two sequential reactions over a bifunctional catalyst. First, CO_2 and H_2 are converted to CH_3OH over a partially reduced oxide surface (e.g., Cu, In, and Zn) or noble metals via a CO or formate pathway. Then, methanol is dehydrated or coupled over zeolites or alumina. Accordingly, bifunctional or hybrid catalysts are composed of a CH_3OH synthesis catalyst and a CH_3OH dehydration/coupling catalyst, which can convert CO_2 into high-value C_{2+} compounds, including DME, hydrocarbons like gasoline, and light olefins. An efficient catalyst for these high-value C_{2+} products should be active for both CH_3OH synthesis and dehydration/coupling under the same conditions (Fig. 1a, R1–R4).

$$CO_2 + 3H_2 \rightarrow CH_3OH + H_2O \quad (R1)$$

$$2CH_3OH \rightarrow CH_3OCH_3 + H_2O \quad (R2)$$

$$nCH_3OH + H_2 \rightarrow CH_3(CH_2)_{n-2}CH_3 + nH_2O \quad (R3)$$

$$nCH_3OH \rightarrow CH_2{=}CH(CH_2)_{n-3}CH_3 + nH_2O \quad (R4)$$

In CO_2 hydrogenation to C_{2+} compounds, the reactions of CO_2 to CH_3OH and CH_3OH to C_{2+} compounds take place at 200–300 °C and 400 °C, respectively, over bifunctional catalysts. Therefore, investigation of the reaction conditions, catalyst properties, and catalytic performance for CO_2 to CH_3OH and CH_3OH to C_{2+} products is necessary.

Methanol. As mentioned earlier, one of the possible targets of CO_2 hydrogenation is to convert CO_2 to CH_3OH. Significant progress has been made in this area recently, especially in developing copper (Cu)- and indium (In)-based catalysts[30,31]. Recent publications have dealt with Cu–ZnO composites, whose CH_3OH selectivity ranges from 30 to 70% at CO_2 conversions less than 30% under typical reaction conditions (temperature: 220–300 °C, pressure <5 MPa, $H_2/CO_2 = 3$)[32,33]. By increasing the pressure to 36 MPa and H_2/CO_2 molar ratio to 10, the single pass CO_2 conversion can be increased to 95.3% with 98.2% methanol selectivity over a Cu–ZnO–Al_2O_3 catalyst[34]. When Cu nanoparticles (NPs) are encapsulated in metal organic frameworks (MOFs) and strongly interact with their secondary structural units, the resultant metal NPs@MOFs (e.g., Cu ⊂ UiO-66[35] and CuZn@UiO-bpy[36]) show enhanced activity and 100% CH_3OH selectivity, while preventing the agglomeration of the Cu NPs. In addition, ZrO_2 is a noted promoter or support in Cu-based catalysts for CTM hydrogenation[37,38].

Indium-based materials have shown promise as alternatives for CO_2 conversion to methanol. Pure In_2O_3 can convert 7.1% of CO_2 with 39.7% selectivity to CH_3OH at 330 °C and 5 MPa[39]. A Pd/In_2O_3 catalyst with many interfacial sites and oxygen vacancies enhances CO_2 adsorption, achieving CO_2 conversions of above 20% with a methanol space time yield (STY) of 0.89 $g_{MeOH}\ g_{cat}^{-1}\ h^{-1}$ at 300 °C and 5 MPa[31]. In_2O_3/ZrO_2 catalysts significantly boost the methanol selectivity to 99.8%, with a CO_2 conversion of 5.2% and long-term stability of 1000 h under industrially relevant conditions[40]. Besides the Cu and In-based catalysts, great progress has also been achieved with ZnO–ZrO_2 solid solution catalysts, as well as Pd/Pt-based catalysts[41–43]. The ZnO–ZrO_2 solid solution catalysts have achieved CH_3OH selectivities of 86–91% under a GHSV of 24,000 $mL\ g^{-1}\ h^{-1}$ with high thermal stability after being tested for more than 500 h; it also shows a strong resistance to sulfur-containing molecules[31]. In 2014, Norskov's group reported a Ni–Ga bimetallic catalyst for CO_2 hydrogenation to CH_3OH at 0.1 MPa, whose STY reached 0.64 $g_{MeOH}\ g_{cat}^{-1}\ h^{-1}$ at 210 °C[44]. Subsequently, a series of noble metal based catalysts, such as Ga–Pd[45], Au–CeO_X/TiO_2[46], and Pt–MoO_X/Co-TiO_2[47], were developed to convert CO_2 to CH_3OH at low pressure or low temperature. Similarly, Fan's group achieved low-pressure CH_3OH synthesis via another series of multiple-metal catalysts that included In_2O_3, like Ni–In–Al/SiO_2 and La–Ni–In–Al/SiO_2, starting with a phyllosilicate precursor[3,48], and achieving CH_3OH STYs of above 0.011 $g_{MeOH}\ g_{cat}^{-1}\ h^{-1}$ at 255 °C and 0.1 MPa.

Dimethyl ether (DME). There has been rapid development in DME synthesis from CO_2 hydrogenation using CH_3OH synthesis catalysts hybridized with CH_3OH coupling catalysts[15]. The effect of promoters, supports, and synthesis conditions have been explored[42,43,49]. For example, the acidic sites on γ-alumina surfaces and the $CuAl_2O_4$ spinel phase can be regulated by promoters like gallium or zinc oxides, resulting in higher stability for Cu NPs during CO_2-to-DME[49]. To date, CO_2 conversion and DME selectivity mostly vary between 35–80% and 5–50%, respectively[15], but CO_2 conversion can reach up to 97% at 280 °C over a Cu–Zn–Al/HZSM-5 catalyst by drastically increasing the reaction pressure (to 36 MPa)[34]. In addition, interesting results

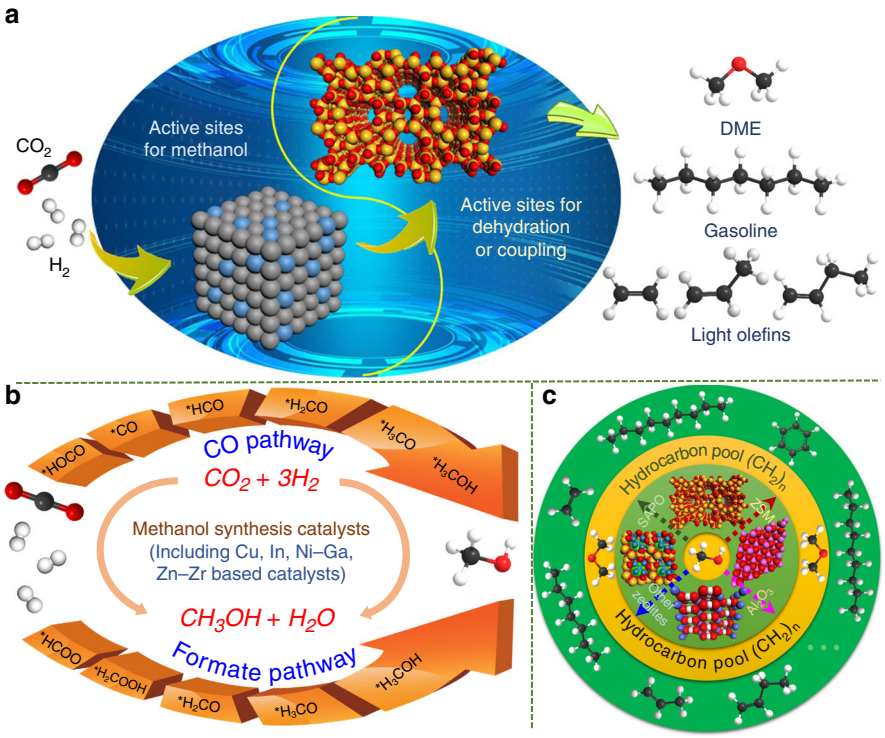

Fig. 1 CO_2 hydrogenation to fuels and chemicals via the methanol reaction mechanism. a Schematic for the reaction mechanism of direct CO_2 hydrogenation to C_{2+} products over bifunctional catalysts. **b** Two possible reaction pathways for methanol synthesis. **c** Schematic for methanol conversion into hydrocarbons inside zeolites via the hydrocarbon-pool mechanism.

have been reported on core–shell structured hybrid catalysts with the MeOH synthesis catalysts at the core and the MeOH dehydration catalysts forming the shell[50,51]. Compared with traditional hybrid catalysts prepared by physically mixing the components, these novel core–shell catalysts have received much attention in the literature due to their unique structures and ability to valorize CO_2 by improving conversion and DME selectivity.

Light olefins, aromatics, and gasoline. MeOH can not only be dehydrated to DME, but also serve as an intermediate to synthesize hydrocarbon chains, $(CH_2)_n$, and final products, such as olefins, aromatics, and gasoline. As mentioned above, defective indium oxide (In_2O_3) with oxygen vacancies is shown to be effective for CO_2 hydrogenation to CH_3OH, while In_2O_3 mixed with SAPO-34 is attractive for efficient CO_2 conversion to CH_3OH and subsequent selective C–C coupling of CH_3OH to form light olefins[52]. The addition of Zr into In_2O_3 is helpful for creating more oxygen vacancies, enhancing CO_2 chemisorption and stabilizing both surface intermediates and active In NPs[53,54]. Similarly, a high yield of light olefins can also be achieved by composite catalysts, such as ZnZrO[16], ZnGaO[55], and CuZnZr[56] mixed with SAPO-34. As shown in Table 1 (Entries 1–5, 9–13), the selectivity of light olefins, represented by the C_2–$C_4^=$ column in the table, can be as high as 90%, while the CH_4 selectivity is less than 5% of the hydrocarbon products with 15–30% CO_2 conversions over most bifunctional catalysts tested, which deviates from the Anderson–Schulz–Flory (ASF) distribution.[52,54] This result is a significant breakthrough in the synthesis of light olefins. When the zeolite is changed from SAPO-34 to HZSM-5, more C_{5+} compounds are produced than light olefins. A 78.6% selectivity of gasoline-range hydrocarbons, with only 1% CH_4 selectivity, was obtained from the tandem In_2O_3/HZSM-5 catalyst[26]. When In_2O_3 is replaced by $ZnAlO_x$ or ZnZrO, CH_3OH is synthesized on the metal oxide surface and then converted to olefins and aromatics inside the HZSM-5 pores with an aromatic selectivity of 73%, which is attributed to a shielding of the external Brønsted acid sites of HZSM-5 by $ZnAlO_x$[57]. Therefore, the type of product is affected by both the character of the metal oxides and the geometries of the zeolites that determine the confinement of the hydrocarbons. Furthermore, as mentioned previously, catalysts with product yields exceeding the ASF distribution limit were recently reported that follow the methanol reaction mechanism-based CO/CO_2 hydrogenation. However, fundamental understanding of this ASF distribution deviation is still lacking. Jiao et al.[58] observed that ketene (CH_2CO) can be formed from the reaction between surface CO and CH_2 species, blocking the surface polymerization, and thus breaking the ASF distribution. Another important reason suggested for the reported ASF distribution deviation is the use of bifunctional catalysts with two types of active sites.

Reaction mechanisms. For most catalysts, the rate-determining step for methanol synthesis is CO_2 activation (R1)[59,60], which includes chemisorption of CO_2 and electron transfer from the catalyst to CO_2[11,61]. Density functional theory (DFT) calculations have shown that different catalysts activate CO_2 through electron transfer between different orbitals[62]. For example, in PtCo-based catalysts, carbon in the CO_2 tends to bind to the Pt sites with an η^1-C_{Pt} bonding mode, while the O in the CO_2 prefer to combine with the reduced $M^{\delta+}$ cations in metal oxides with η^1-$OM^{\delta+}$ configuration[63]. In addition, oxygen vacancies on metal oxide surfaces and Lewis acid sites have also been shown to enhance CO_2 activation[37,55], stabilize intermediates[64], and reduce sintering[52]. DFT calculations reveal that an oxygen-defective surface could be created through direct thermal desorption or exposure to a reducing agent[54]. After activation, CO_2 proceeds to form methanol, most likely via a formate intermediated pathway.

Table 1 Representative catalysts and their performance for hydrogenation of CO_2 to C_{2+} species.

Entry	Catalysts	CO_2 con./%	CO select./%	CH select./%	Hydrocarbon distribution/%[a]				GHSV/ml g^{-1} h^{-1}	Temp./°C	P/MPa	Ref.
					CH_4	C_2-C_4^0	C_2-$C_4^=$	C_{5+}				
C_{2+} hydrocarbons based on methanol reaction mechanism												
1	In_2O_3/ZrO_2+SAPO-34	19.0	87.0	13.0	4.0	12.0	84.0	-	3000	400	1.5	53
2	In_2O_3/SAPO-34	15.3	68.3	31.7	2.7	13.7	81.9	1.7	9000	380	3.0	52
3	In_2O_3-ZrO_2/SAPO-34	26.2	63.9	36.1	2.0	21.5	74.5	2.0	9000	380	3.0	52
4	In-Zr/SAPO-34	29.0	78.2	-	4.1	9.2	83.9	2.8	15,750	400	3.0	54
5	ZnZrO/SAPO-34	12.6	47.0	-	3.0	14.0	80.0	3.0	3600	380	2.0	16
6	(CuO-ZnO)-Kaolin/ SAPO-34	50.4	7.5	-	13.6	15.8	70.6	0.0	1800	400	3.0	145
7	Zn-Ga-O/SAPO-34	13.0	46.0	-	1.0	11.0	86.0	2.0	5400	370	3.0	55
8	CuZnZr@Zn-SAPO-34	19.6	58.6	41.4	14.6	20.2	60.5	4.8	3000	400	2.0	56
9	In_2O_3/HZSM-5	13.1	44.8	-	1.0	-	-	78.6	9000	340	3.0	26
10	Cr_2O_3/HZSM-5	33.6	41.2	-	3.0	15.7	3.1	78.2	1200	350	3.0	146
11	Fe_2O_3/HZSM-5	7.1	73.5	-	2.0	-	-	70.5	9000	340	3.0	26
12	$ZnAlO_x$ and HZSM-5	9.1	57.4	42.6	0.5	6.7	10.7	80.3	2000	320	3.0	57
13	ZnZrO/HZSM-5	14.1	43.7	57.3	0.3	14.5	4.9	80.3	1200	320	4.0	71
C_{2+} hydrocarbons based on CO_2 modified FTS mechanism												
14	FeZnK-NC	34.6	21.2	78.8	24.2	7.1	40.6	28.1	7200	320	3.0	120
15	Fe-2K	~30.0	22.0	74.0	31.1	14.9	32.4	21.6	-	320	2.0	82
16	10Fe0.8K0.53Co	54.6	2.0	98.0	19.3	7.8	24.9	48.0	560	300	2.5	91
17	N-K-600-0	43.1	26.1	73.9	35.5	6.8	36.9	20.8	3600	400	3.0	121
18	1Fe-1Zn-K	51.0	6.0	85.1	34.9	7.8	53.6	3.7	1000	320	0.5	147
19	35Fe-7Zr-1Ce-K	57.3	3.1	96.3	20.6	7.9	55.6	15.9	1000	320	2.0	76
20	Fe-Co/K-Al_2O_3	41.4	14.8	85.2	21.7	6.3	45.0	27.0	9000	320	3.0	77
21	C-Fe-Zn/K	54.8	4.6	94.4	23.1	8.5	57.4	11.0	1000	320	2.0	78
22	Na-Fe_3O_4/HZSM-5	22.0	20.1	-	4.0	-	-	79.4	4000	320	3.0	17
23	$ZnFeO_x$-4.25Na/ S-HZSM-5	36.2	11.0	89.0	8.2	13.3	3.2	75.4	4000	320	3.0	93
24	Fe-Cu-K-La/TiO_2	23.1	33.0	67.0	19.4	-	-	67.2	3600	300	1.1	115
25	Na-$ZnFe_2O_4$	34.0	11.7	-	9.7	-	-	58.5	1800	340	1.0	116
26	K-Fe	43.9	10.1	89.9	12.2	-	-	56.6	750	300	1.5	148
27	92.6Fe7.4 K	41.7	6.0	94.0	10.9	23.0	6.5	59.6	560	300	2.5	122
28	10Fe4.8 K	35.2	9.0	91.0	8.1	4.3	16.4	71.2	560	300	2.5	91
29	$CuFeO_2$−24	16.7	31.4	-	2.4	-	-	64.9	1800	300	1.0	123
30	Na-CoCu/TiO_2	18.4	30.2	-	26.1	-	-	42.1	3000	250	5.0	96
31	Co/MIL-53(Al)	25.3	6.6	18.7	35.2	-	-	35.0	800	260	3.0	94

Entry	Catalysts	CO_2 con./%	CO select./%	HC select./%	MeOH select./%	C_{2+}OH select./%	GHSV/ml g^{-1} h^{-1}	Temp./°C	P/MPa	Ref.
C_{2+} alcohols from CO_2 hydrogenation										
32	$CuZnFe_{0.5}K_{0.15}$	42.3	6.9	56.4	4.7	32.0, C_{2+}OH	5000	300	6.0	99
33	$Mo_1Co_1K_{0.8}$ sulfide	28.8	-	-	70.9	10.9, C_{2+}OH	3000	320	5.0	149
34	1 wt%Pt/Co_3O_4	-	-	-	-	82.5, C_{2+}OH	-	200	8.0	98
35	PdCu NPs/P25	-	-	-	-	92.0, EtOH	-	200	3.2	150
36	RhFeLi/TiO_2	15.7	12.5	53.9	2.2	31.3, EtOH	6000	250	3.0	18

[a]The hydrocarbon distribution was calculated without CO

The use of DFT and ab initio molecular dynamics sampling techniques on Cu–ZnO[32], Cu–Pd[42,65], In[66], and Ga[48,67] catalysts suggest that methanol synthesis occurs via a formate intermediate (See Fig. 1b). However, while calculations for Cu–ZnO interfacial sites suggest a formate intermediate[32], calculations for the near surface regions suggest a CO intermediated pathway[68]. In addition, the calculations indicate that H_2O produced in situ from both RWGS and CH_3OH formation on Pd incorporated Cu catalysts accelerates CO_2 conversion to methanol by reducing the kinetic barriers by 0.2–0.7 eV for O–H bond formation steps[42,65]. On In-based catalysts, defective In_2O_3 surfaces have different CO_2 activation barriers[66]. The synthesized methanol can then be transformed into high-value C_{2+} compounds, including DME, lower hydrocarbons, and gasoline via the hydrocarbon-pool mechanism in which an organic center is trapped in the zeolite pores and acts as a co-catalyst, as depicted in Fig. 1c[26,69,70]. The DFT results indicate that the rate-determining step is generally CO_2 activation during conversion to methanol over the hybrid catalysts, whose ΔG^0 at 320 °C reaches 47 kJ/mol, which is much higher than that of the subsequent dehydration reaction (e.g., $\Delta G^0 = -87$ kJ/mol for methanol to xylene at 320 °C)[71,72]; thus, an efficient CH_3OH synthesis catalyst is beneficial for the subsequent formation of C_{2+} compounds.

As indicated above, the bifunctional catalysts consist of CH_3OH synthesis and dehydration catalysts. However, is the bifunctional catalyst mechanism also the simple sum of the two individual reactions? Li et al.[16] estimated the CH_3OH selectivity based on the hydrocarbon selectivity for a hybrid catalyst and found that it was much higher than that for ZnZrO alone. This result clearly indicates that the products from the bifunctional catalysts are not a simple sum of the two individual reactions, and these two catalysts have a large synergistic effect. Thus, further

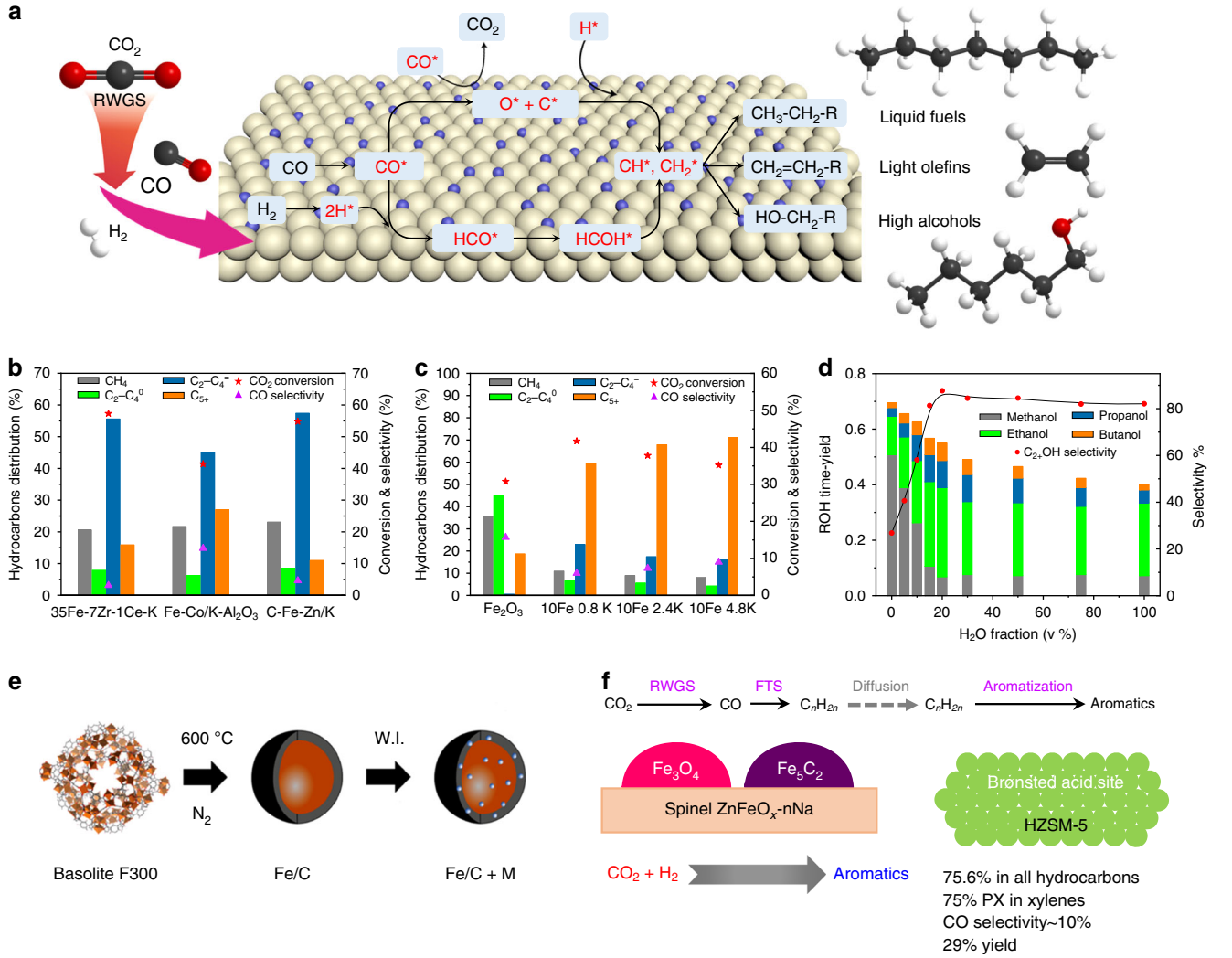

Fig. 2 CO_2 hydrogenation to C_{2+} products via the FTS-based mechanism. a Scheme of CO_2 modified FTS-based catalytic mechanism. **b**–**d** CO_2 hydrogenation via the FTS mechanism for production of light olefins, liquid fuels, and higher alcohols[76–78,91,98]. **e** Synthesis strategy for an Fe-based catalyst. (Reprinted with permission from Ramirez et al.[83]. Copyright (2018) American Chemical Society). **f** Selective production of aromatics from the CO_2 hydrogenation process over a $ZnFeO_x$-*n*Na/HZSM-5 catalyst. (Reprinted with permission from Cuiet al.[93]. Copyright (2019) American Chemical Society).

study on the direct CO_2 hydrogenation to C_{2+} products over bifunctional catalysts is still desirable.

Fischer–Tropsch synthesis (FTS)-based CO_2 hydrogenation

Heterogeneous FTS-based CO_2 hydrogenation can be realized in either one or two reactors, although the single reactor process dominates. The direct one-reactor conversion system has drawn much attention due to its ease of operation and thus lower CO_2 conversion cost. This process integrates the reduction of CO_2 to CO via the RWGS reaction and hydrogenation of CO to hydrocarbons via FTS. An efficient catalyst for generating C_{2+} products, which generally refer to light olefins, liquid fuels, and higher alcohols, should be active for both RWGS and FTS under the same conditions (Fig. 2a, R5–R7). The product distribution can be wide, depending on the structure and composition of the catalysts. Iron (Fe), cobalt (Co), and ruthenium (Ru) based supported catalysts, with appropriate promoters, are predominantly used in this area.

$$nCO_2 + (3n+1)H_2 \rightarrow C_nH_{2n+2} + 2nH_2O \quad (CO_2\ \text{Hydrogenation}) \quad (R5)$$

$$\Delta_R H_{573K} = -128\,\text{kJ/mol}$$

$$CO_2 + H_2 \rightarrow CO + H_2O \quad (\text{RWGS}) \quad (R6)$$

$$\Delta_R H_{573K} = 38\ \text{kJ/mol};$$

$$nCO + (2n+1)H_2 \rightarrow C_nH_{2n+2} + nH_2O \quad (\text{FTS}) \quad (R7)$$

$$\Delta_R H_{573K} = -166\,\text{kJ/mol}$$

(The values of $\Delta_R H$ are reproduced from the literature[73,74]).

Prior to FTS, the RWGS reaction converts CO_2 to CO to form dissociatively adsorbed *CO precursor molecules on the catalyst surface. Therefore, an understanding of the reaction conditions and catalytic performance for the RWGS reaction is necessary. Since RWGS (R6) is endothermic, it requires high temperatures for reasonable conversions. CO selectivity up to 100% can be achieved at 200–600 °C using the primary RWGS catalysts, such as Cu- and noble metal (Pt, Pd, Rh)-based catalysts, with CO_2 conversions up to 50%[75].

Light olefins. Light olefins, including C_2–C_4 alkenes, are important target products for the FTS-based CO_2 hydrogenation process. Fe-based catalyst systems are considered to be most suitable for olefin production by applying appropriate promoters, textural additives, or supports to form the required active sites for the different reaction stages. Fe and Co-based catalysts with alkali metal promoters (e.g., 35Fe–7Zr–1Ce–K[76], Fe–Co/K–Al_2O_3[77], and C–Fe–Zn/K[78]) are reported to be highly active for FTS to produce C_{2+} products[79,80] with as high as 57% selectivity at 40–60% CO_2 conversion (Fig. 2b). The most effective promoters are alkali metals, especially Na and K, as they limit the formation of methane while improving the selectivity to C_{2+} products[81]. Meiri et al.[82] pointed out that the introduction of potassium can stabilize the texture of the Fe–Al–O spinel, increase the surface content of Fe_5C_2, and strengthen CO_2 adsorption. In one study of fourteen different kinds of promoters added individually to MOF-derived Fe/C catalysts (Fig. 2e), only K dramatically enhanced the olefin selectivity from 0.7 to 36%[83]. Martinelli et al.[84] concluded that the K-loading did not influence the CO_2 conversion, but increased the olefin/paraffin ratio and the average molecular weight of the products. Besides the alkali metals, other metals such as Cu, Zn, Ni, Zr, Mn, and Pt can also be used to modify Fe-based catalysts[83]. For example, bimetallic Fe–Cu/Al_2O_3 catalysts can suppress CH_4 formation and thus exhibit higher amounts of C_2–C_7 production compared with pure Fe/Al_2O_3 catalysts[85].

Support material is another important factor that can influence catalyst activity and product selectivity by affecting the dispersion of active metals and the interactions between reactive intermediates and the support material. The support materials for Fe-based FT catalysts can be divided into metal oxides (e.g., ZrO_2, CeO_2, and Al_2O_3) and carbonaceous materials (e.g., MOFs, mesoporous carbon, carbon nanotubes (CNTs), graphene, and organic precursors to mesoporous carbon). Wang et al.[86] studied several supports and found that a ZrO_2 supported (K-Fe/ZrO_2) catalyst exhibited the highest selectivity to lower olefins, while SiO_2 was not suitable for the CO_2-FTS reaction. Since Fe carbides are generally considered to be the active phase in FTS catalysis, carbon materials are naturally considered as good support materials for Fe catalysts; indeed, they have demonstrated excellent catalytic performance for olefin synthesis. Carbon support materials can improve the dispersion of the active metals and lead to higher selectivity to olefins[87]. An Fe-based core–shell nanocatalyst with Fe_3O_4 and Fe_5C_2 in the core and partially graphitized carbon in the shell was prepared to efficiently convert CO_2 to C_2–$C_4^=$ olefins. The olefin/paraffin ratio was increased by carefully controlling the content of carbon to improve the accessibility of reactants to the active sites[88]. CNTs and graphene are also good carbon supports with superior thermal and chemical stability[87,89]. For example, a honeycomb-structured graphene (HSG) with a special meso-macroporous architecture was devised to confine K-promoted Fe NPs for the CO_2-to olefins reaction. The FeK1.5/HSG catalyst can increase the selectivity of C_2–$C_4^=$ to 59.0% and the stability to 120 h, due to K promotion and HSG confinement effects[89]. Similarly, Ding et al. have successfully improved the catalytic activities by combining the K promoter and ZrO_2 support with sufficient oxygen defects[90].

C_{5+} products. Liquid fuels (e.g., gasoline and diesel) and other value-added chemicals (e.g., aromatics and isoparaffins) are also desired products from CO_2 hydrogenation via FTS. Jiang et al.[91] prepared Fe- and FeCo-based catalysts and achieved, when promoted with an appropriate amount of K, ≥54.6% CO_2 conversions and ≥47.0% C_{5+} selectivity (Fig. 2c). A Na–Fe_3O_4/HZSM-5 catalyst with three types of active sites was developed by Wei et al., demonstrating that 22% of CO_2 can be directly converted to gasoline with a selectivity of 78%[17]. When HZSM-5 was changed to HMCM-22, aromatization was suppressed, while isomerization was promoted due to the appropriate Brønsted acid properties of HMCM-22 and the special lamellar structure consisting of two independent pore systems. Thus, 57% selectivity of isoparaffins was obtained over the Na–Fe_3O_4/HMCM-22 catalyst, while the values over Na–Fe_3O_4/HZSM-5 and Na–Fe_3O_4 were only 34 and 6%, respectively[92]. Similarly, aromatics are important feedstocks with applications in the synthesis of various polymers, petrochemicals, and medicines. $ZnFeO_x$–nNa/HZSM-5 catalysts can achieve 75.6% selectivity to total aromatics at a CO_2 conversion of 41.2% (Fig. 2f)[93].

Owing to superior ability for chain growth, stability, and lower activity for the WGS reaction, Co-based catalysts have also been applied to produce long-chain C_{5+} hydrocarbons. Recently, a pure Co-based catalyst without promoters was reported to display high performance for both CO-FTS and CO_2-FTS[94,95]. The Co/MIL-53(Al) catalyst was first found to exhibit 47.1% CO conversion and 68.6% selectivity to C_{5+} products. When it was applied to CO_2-FTS, 35.0% selectivity to C_{5+} was still achieved at 260 °C. Furthermore, different kinds of promoters and support materials are employed to tune the product distribution towards heavier hydrocarbons. Shi et al. prepared a promoted Co–Cu bimetallic catalyst for CO_2 hydrogenation based on consideration of Cu as a popular RWGS catalyst. For example, with the introduction of Na as a promoter to a CoCu/TiO_2 catalyst, the CH_4 selectivity significantly decreased from 89.5 to 26.1%, while the C_{5+} selectivity increased from 4.9 to 42.1%, with an excellent stability of more than 200 h[96]. He et al.[97] reported the bimetallic Co_6/MnO_x nanocatalyst with synergism between Co and Mn for 15.3% CO_2 conversion and 53.2% C_{5+} selectivity.

Higher alcohols. Reports of higher alcohol (C_{2+}OH) production are less prevalent compared to methanol and other C_{2+} products of CO_2 hydrogenation. However, C_{2+}OH alcohols have higher energy density and wider applications as fuel additives. The formation of higher alcohols is a parallel reaction competing with formation of hydrocarbons during the FTS process, resulting in much lower selectivity to C_{2+}OH. Furthermore, the synthesis of C_{2+}OH is difficult, as both C–C coupling and OH formation are required. Interestingly, water was found to enhance the selectivity of higher alcohols to 82.5% over a 1 wt% Pt/Co_3O_4 catalyst (Table 1, Entry 34)[98]. Moreover, the C_{2+}OH selectivity was affected by the volume fraction of water, increasing dramatically with small amounts (<20 vol%) of added water, and then decreased slightly with further addition of water (Fig. 2d). The promoting effect of water was attributed to assisting methanol dissociation to form more *CH_3 species. *CH_3 then can react with *CO to form *CH_3CO, which will be further hydrogenated to ethanol (EtOH). Also, ordered Pd–Cu NPs, with charge transfer between Pd and Cu, are reported to efficiently convert CO_2 to ethanol with 92.0% selectivity (Table 1, Entry 35). The rate-determining step of *CO hydrogenation to *HCO can be promoted on a Pd–Cu NPs/P25 catalyst, leading to lower *CO coverage and weaker *CO adsorption. Similarly, Cu–Fe and Zn–Fe interactions in the Fe-doped K/Cu–Zn catalyst have synergistic interactions, which can facilitate catalyst reduction and metal dispersion, as well as increase the yield of higher alcohols[99]. The reduction temperature can be regulated to obtain different phase compositions over the Co-based catalysts. For example, an alumina-supported catalyst reduced at 600 °C ($CoAlO_x$−600) contained coexisting Co–CoO phases and exhibited 92.1% selectivity to ethanol at 140 °C, due to the formation of acetate intermediates from formate by insertion of *CH_x[100].

Reaction mechanisms. Although many successful catalysts have been developed for the CO_2-FTS reaction, the nature of the active sites and reaction mechanism remain controversial. In view of the catalysts reported to date, the mechanism of the RWGS reaction can be assigned to either the decomposition of *HOCO intermediates or to direct C–O bond cleavage to produce *CO[75]. Ko et al.[101] pointed out that CO_2 can be activated to anionic $CO_2^{\delta-}$ through charge transfer from the pure and bimetallic alloy surfaces with bending of the structure and splitting of the π orbital. Both the adsorption energy of $CO_2^{\delta-}$ and the reaction energy for CO_2 dissociation are a linear function of adsorption energies of *CO and *O. To facilitate further *CO hydrogenation, the interaction between *CO and the catalyst interface need to be enhanced; otherwise, *CO is desorbed with concomitantly increased CO selectivity. According to the most-accepted reaction mechanism, during the FTS process, steps including *CO dissociative chemisorption on the active sites with hydrogen-assisted insertion to form $*CH_x$ intermediates, initiation of chain growth through the coupling of $*CH_x$, and the termination of chain growth through further hydrogenation, dehydrogenation, or insertion of non-dissociatively adsorbed *CO happen successively on the catalyst surface (Fig. 2a). *CO intermediates can be produced through the RWGS reaction, followed by the FTS reaction. According to modeling and kinetic analysis by Willauer et al., the RWGS reaction rate can reach $3.5 \times 10^5\ s^{-1}$ initially and decreases to $0.032\ s^{-1}$ within 2 s, while the FTS reaction rate is zero initially and increases to $0.004\ s^{-1}$ at 18.7 s[102]. The FTS reaction is the rate-limiting step due to the much lower reaction rate. The FTS reaction during the CO_2 hydrogenation process is limited by the reaction between the adsorbed CO and H_2 to form *HCO intermediates, as reported by Pour et al.[103] after evaluating different kinetic models and applying a genetic algorithm (GA) approach and the Levenberg–Marquardt (LM) method. Thus, efficient active sites for the FTS reaction are important for the whole CO_2 hydrogenation process. Also, chain propagation in FTS is still in dispute based on the basic C–C coupling mechanisms[104]. The most limiting process or factor during FTS-based CO_2 hydrogenation that should be addressed in future research may be affected significantly because of the various thermodynamic and physical properties of the reactions. For example, when using higher reaction temperatures (>300 °C), mass transfer appears to become the rate-limiting step instead of the surface reaction at relatively low temperatures[105].

Concerning the active sites in iron and cobalt catalysts, several phases are present and change dynamically during reaction. The catalyst transformation in structure and composition has several steps with their own kinetic regimes[106]. The reduced iron catalysts mainly consist of α-Fe and Fe_3O_4 with extremely low activity at the beginning of FTS. Fe_3O_4 is capable of activating CO_2 to CO via the RWGS reaction[81,107]. Then, the α-Fe reacts with the dissociatively adsorbed CO to form iron carbide (e.g., Fe_5C_2), generating Fischer–Tropsch activity. Thus, the catalytic sites of iron carbides appear to be active for CO activation and chain growth[81]. Considering the different functions of iron species and the zeolites' superior properties of acid sites for oligomerization/aromatization/isomerization, a multifunctional structure Na–Fe_3O_4/HZSM-5 catalyst was developed and achieved as high as 78% selectivity to gasoline, with only 4% methane generated[17]. Therefore, researchers need to focus not only on optimizing the composition and structure of the catalysts, but also on developing new catalytic systems with desired properties by using comprehensive approaches that can directly control the microstructures of the catalysts and be used for more accurately identifying the reaction pathways during FTS-based CO_2 hydrogenation.

It is generally accepted that bulk Fe catalysts show insufficient catalytic performance and that the addition of promoters can enhance the selectivity to C_{2+} products. However, the essential basis of the promotion effect remains unclear. More investigation needs to focus on the reaction mechanism. For example, the reaction pathways over Fe/Al_2O_3, Cu/Al_2O_3, and Fe–Cu/Al_2O_3 catalysts are different, resulting in different product distributions[85]. Cu has high activity for the RWGS reaction instead of the CO_2 methanation reaction, leading to more surface *CO. Thus, bimetallic Fe–Cu/Al_2O_3 catalysts form more CO, which leads to more C_{2+} hydrocarbons compared to the Fe/Al_2O_3 catalyst. Nie et al. also investigated the mechanism of CO_2 hydrogenation to methane and C_2 hydrocarbons over Fe(100) and Cu–Fe(100) surfaces and showed that the hydrogenation barrier of CH_2* species is higher than those for C–C coupling and CH–CH* conversion to ethylene on Cu–Fe bimetallic catalysts (see Fig. 3)[108], which results in a more selective process to ethylene. The addition of K to Fe–Cu/Al_2O_3 catalysts can further inhibit methanation and enhance the production of olefin-rich C_2–C_4 hydrocarbons by increasing the surface coverage of carbon[85]. DFT calculations show that the presence of K on Fe-based surfaces can enhance the CO_2 adsorption strength and reduce the CO_2 dissociation barrier (e.g., 2.36 eV for oct2-Fe_3O_4(111) versus 1.13 eV for K/oct2-Fe_3O_4(111))[109]. Therefore, the introduction of promoters can modify the surface electronic features.

Outlook

Methanol reaction based CO_2 hydrogenation. The primary challenge in converting CO_2 to value-added products is low selectivity due to excessive formation of CO and the large amount of water (H_2O) generated. CO and CH_4 are both formed due to partial reduction and cracking, respectively, during dehydration at the elevated temperatures (≥400 °C) generally employed for dehydration. To date, it has limited conversion (<30%) towards desired products (Table 1, Entries 1–5, 7–13). In addition, H_2O produced from CH_3OH synthesis and dehydrative coupling further complicates separations and, in some cases, deactivates the catalyst. However, altering the zeolite structure has been shown to alter product distributions and increase selectivity to desired products, which was realized by increasing the space velocity during catalytic CO_2 hydrogenation over In_2O_3 combined with zeolites[26,110]. Through the introduction of CO conversion promoters, such as In–FeK, In–CoNa, or CuZnFe/zeolites, bifunctional catalysts can be upgraded to reduce CO formation. In addition, these catalytic CO_2 conversion technologies face several other challenges, such as revealing the relationship between product type and molecular sieve type, increasing the CO_2 conversion and final product yield via improving the structures of bifunctional catalysts, as well as further elucidating the reaction mechanisms. More detailed information on these points is depicted below.

First, more research on the zeolite properties is needed. By varying the zeolite structure, the product distribution can be better controlled. For example, HZSM-5 zeolite is selective towards DME and gasoline, whereas SAPO molecular sieves are preferred for light olefin generation. However, the structure-property relations between zeolite properties and CO_2 hydrogenation activity have not yet been systematically investigated. Because many variables and conditions exist during zeolites synthesis (e.g., synthesis template, crystallization temperature, and Si/Al ratio), the relationship between zeolite properties and CO_2 hydrogenation activity remains an active area of study[111–113]. Shape-selective catalysis was identified as a factor in these catalysts, as SAPO zeolite windows allowed only small linear hydrocarbons to pass, while H-ZSM zeolite windows

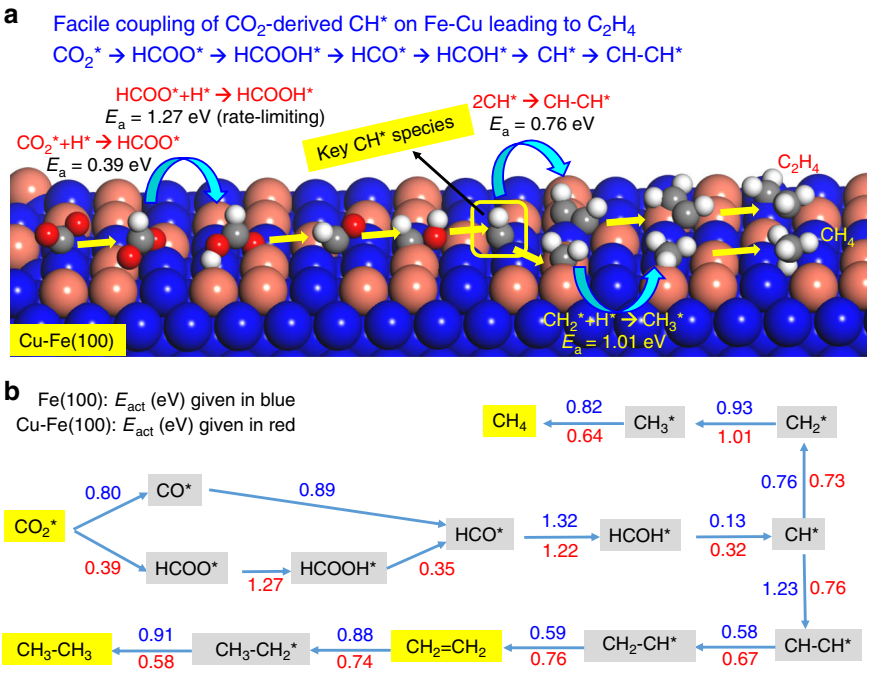

Fig. 3 Mechanistic insight into C–C coupling over Fe-Cu bimetallic catalysts. a Mechanism of CO_2 hydrogenation to C_2H_4 over a Cu–Fe(100) surface. **b** Reaction pathways for production of CH_4, C_2H_4, and C_2H_6 from CO_2 hydrogenation on Fe(100) and Cu–Fe(100) surfaces at 4/9 monolayer coverage. The kinetic barrier for each elementary step is given in eV. (Reprinted with permission from Nie et al. [108]. Copyright (2017) American Chemical Society).

allowed much larger branched and linear hydrocarbons to leave[114]. In addition, DFT calculations have linked density of surface Lewis acids and defects in the zeolite structure with dehydration activity[115,116].

Second, additional research on the structure of bifunctional catalysts is required. To improve CO_2 conversion and final product yield, the morphology and structure of the bifunctional catalysts should be optimized, rather than just making physical mixtures. The precise control of the desired morphology and structure of the catalyst is a significant and synthetically challenging task (see Fig. 4a–c), as shown by the example of utilizing core–shell structures incorporating multiple-metal oxide cores to direct the growth of zeolite shells. Additionally, catalysts with core–sheath and lamellar structures are reported to exhibit high activity and stability for C=O bond hydrogenation[117]. Bifunctional catalysts can be assembled via layer-by-layer growth methods and probably exhibit better performance. Furthermore, efforts to improve important intrinsic factors, like the dispersion and crystallite size of active metals on methanol synthesis catalysts and the acid strength together with acid sites on the zeolites, as well as the methods of integration of the active components, should be made. As shown in Fig. 4d–f, different product distributions were obtained when the methanol synthesis catalyst and the zeolite were synthesized with different spatial arrangements[16,26,71]. The TEM and SEM images in Fig. 4g–i indicate that ZnZrO particles can be highly dispersed on the surface of HZSM-5 and maintain their own structures[16,26,71]. Sufficient physical mixing of the two components seems to be better than the granular form or a dual-bed separated in space by a layer of quartz sand.

Analyzing the integration between methanol synthesis catalysts and zeolites remains a challenge. DFT calculations may be the most efficient method to explore the interactions between CH_3OH synthesis catalysts and dehydration catalysts. However, the information gained from DFT calculations can be limited because the systems studied are under idealized conditions, which are different from the ones in a packed bed reactor. As computing power with machine learning continues to increase, more complex and realistic catalytic systems can be modeled, which provides deep insight into the mechanism of CO_2 hydrogenation to olefins, such as the design of 3D nanocrystal tandem catalysts with multiple interfaces for CO_2 hydrogenation.

FTS-based CO_2 hydrogenation. The major obstacles of FTS-based CO_2 hydrogenation lie in the thermal stability of CO_2 and the complicated reaction mechanism with a wide product distribution. With the RWGS process being endothermic and FTS being exothermic, both need to be efficiently catalyzed under the same conditions, which sets a very strict requirement for the catalytic system. The designed catalysts should be effective for the RWGS reaction and also active enough for the subsequent FTS reaction. Different active sites must be precisely tuned and carefully dispersed on the support materials. These challenges will be discussed in view of different kinds of products: olefins, C_{5+} hydrocarbons, and higher alcohols.

The first, challenge to be discussed is production of light olefins. In spite of the promising results discussed, major challenges still remain. For example, the selectivity of C_2–$C_4^=$ can be above 80% for catalysts with methanol as the reactive intermediate, while only about 50% selectivity to C_2–$C_4^=$ is achieved on the catalysts for CO_2 conversion via FTS (Table 1, Entries 14–21). The key to improve the C_{2+} selectivity is to develop catalysts that have compatible bifunctional active sites for the two reaction steps, namely, *CO generation and subsequent *CO hydrogenation. The appropriately engineered reaction window is extremely important. The consequence of the incompatible activity of these two different types of active sites could be high CH_4 selectivity (~30%, Table 1, Entries 14–21), as is suggested by the activation energy of RWGS being higher than that of CH_4 formation (81.0 and 59.3 kJ/mol, respectively) for Fe-based catalytic CO_2 hydrogenation[105]. As shown in Table 1 (Entries 1–8, 14–23), the reaction temperature (~320 °C) for the CO_2-FTS process is lower than that for the methanol-mediated

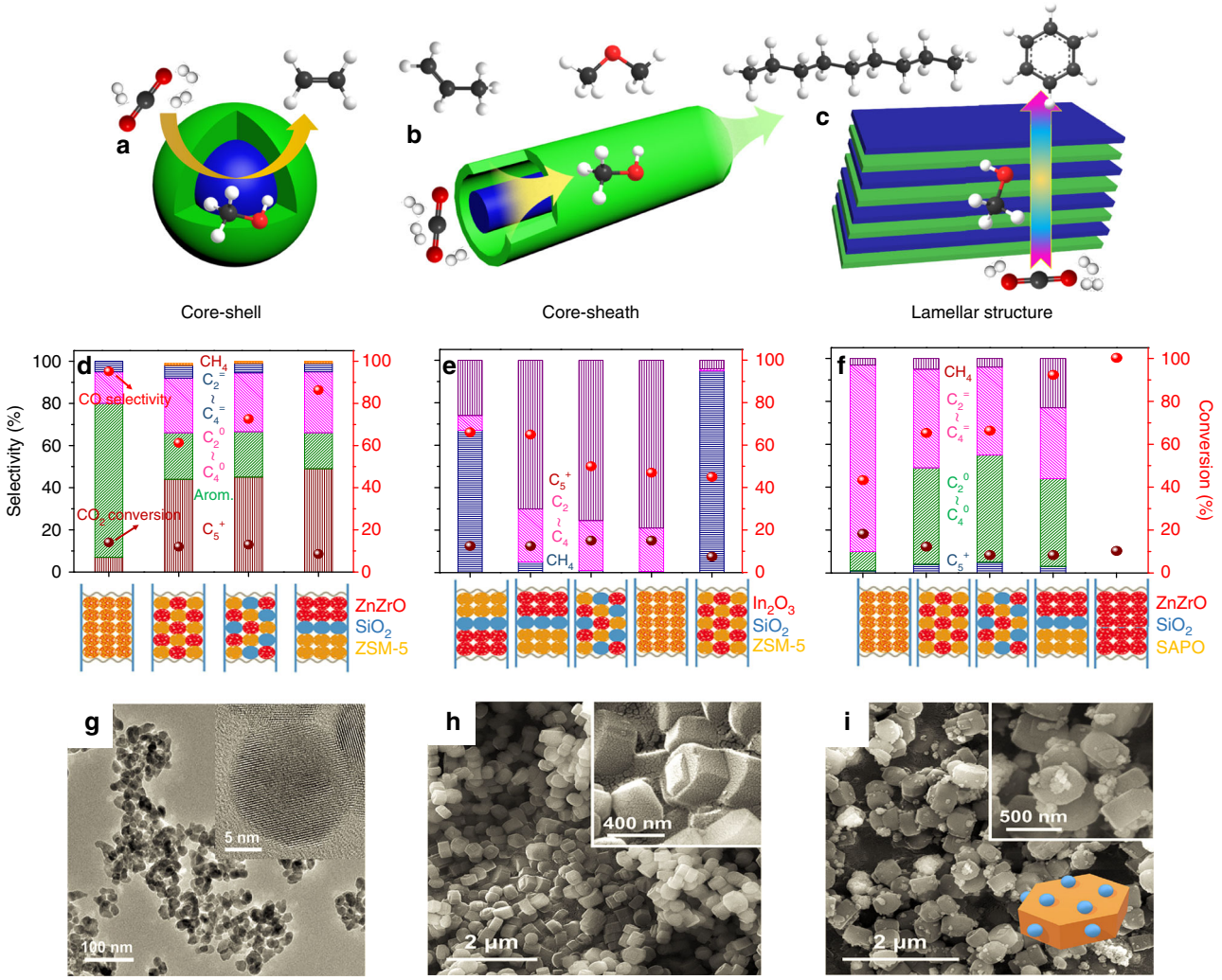

Fig. 4 The structure and performance of bifunctional catalysts. a–c Proposed structures of bifunctional catalysts. **d–f** Hydrogenation of CO_2 over bifunctional catalysts, which are integrated methanol synthesis catalyst and zeolites, with different spatial arrangements. (Adapted with permission from Li et al.[71]. Copyright (2019) Elsevier); Gao et al.[26]. Copyright (2017) Springer Nature; Li et al.[16]. Copyright (2017) American Chemical Society). **g–i** TEM and SEM images of bifunctional catalysts. (Reprinted with permission from Li et al.[71]. Copyright (2019) Elsevier).

route (~380 °C). Thus, the CO selectivity (~30%) is dramatically reduced due to relatively low temperatures for the RWGS reaction, leading to improved hydrocarbon selectivity.

Many researchers have tried to provide possible solutions for improving C_{2+} selectivity by adjusting the structures and compositions of the catalysts. Specifically, development of enhanced promoters, supports, and experimental conditions have been attempted. For example, bulk Fe is favorable for methane formation; however, olefin and long-chain hydrocarbon production can be enhanced with the addition of promoters (i.e., alkaline promoters). Potassium, as an electronic promoter, can regulate the phase proportion of $Fe^0/FeO_x/FeC_x$ to maintain an optimum balance. The dissociative adsorption of *CO can be improved, while surface *H is decreased by donated electrons to the vacant d-orbital of Fe. The resulting higher C/H ratio favors chain growth and chain termination by forming unsaturated hydrocarbons[118]. Thus, a very important challenge is to increase the surface C/H ratio. Competitive adsorption between H_2 and CO occurs on the catalyst surface. The partial pressure of CO is always limited due the difficulty of converting CO_2 via the RWGS reaction. Since a high C/H ratio is desired to form unsaturated hydrocarbons, a possible strategy would be to enhance CO_2 activation and CO adsorption, while weakening H_2 adsorption[101]. In addition, the H_2 ratio in the feed gas should also be carefully chosen. To achieve good results from FTS-based CO_2 hydrogenation, more consideration is needed based on the characteristics of those reactions instead of imitation of the CO hydrogenation process.

To increase selectivity to light olefins, further hydrogenation must be suppressed. Thus, synergy between the promoter and the support is suggested. For example, an Al_2O_3 support can interact with a K promoter to form a $KAlO_2$ phase under calcination temperatures above 500 °C, which has been shown to suppress further hydrogenation of olefins[77]. To increase the synergistic effect, the active metal can be mixed with supports. A series of K-modified supports (activated carbon, TiO_2, ZrO_2, SBA-15, B-ZSM-5, and Al_2O_3) were physically mixed with Fe_5C_2 and tested for direct hydrogenation of CO_2. The Fe_5C_2–10 K/α-Al_2O_3 catalyst converted 40.9% of CO_2 with a selectivity of 73.5% to C_{2+} products, containing 37.3% C_2–$C_4^=$ and 31.1% C_{5+}[119]. A promising support for Fe-based catalysts is MOF-derived carbon materials. Some researchers have recently developed methods of using MOFs to fabricate carbon supported Fe-based catalysts[83,120]. Two Fe-MOF-derived catalysts have been reported for CO_2 hydrogenation, with high stability and selectivity to light olefins and liquid fuels[120,121]. However, the challenge of

separating light olefins from unreacted CO_2 and H_2 remains. Increasingly advanced techniques and materials are required for their separation.

The second, set of challenges are production of C_{5+} products. These challenges are similar to those for the synthesis of light olefins, due to the shared fundamental reaction mechanism. The selectivity of C_{5+} products is also comparable to that of light olefins synthesis (Table 1, Entries 22–31). CO_2 hydrogenation to C_{5+} products consist of multiple steps, including the RWGS reaction, C–C coupling, and acid-catalyzed reactions (oligomerization, isomerization, or aromatization). Therefore, cooperation between steps is required to develop an efficient and multifunctional catalyst. As zeolites are often used to incorporate the active sites, they generally undergo deactivation as a result of coke deposition. For example, the selectivity of isoparaffins over a Na–Fe_3O_4/HMCM-22 catalyst was reduced from ~60 to ~30% and the total acidity of HMCM-22 decreased from 0.200 to 0.032 $mmol_{pyridine}$ g_{cat}^{-1} after 12 h of reaction time, which was attributed to coke formation and accumulation in the cavities and channels[92]. Thus, a big challenge for the synthesis of C_{5+} products is to reduce coke deposition in the zeolites and to enhance the catalyst stability. As heavier hydrocarbons contain many components, it is difficult to precisely control a specific type of product. Zeolites with different framework topologies are suggested to regulate product distribution. In addition, in contrast to the CO-based FTS process, the reaction is fed with stable CO_2 molecules; therefore, the reformation of CO_2 from the produced CO via the WGS reaction is a thermodynamically favorable process, which limits CO_2 conversion[17,122]. One method to decrease the reformation of CO_2 from CO is to develop better multifunctional catalysts by employing appropriate promoters to facilitate the formation of iron carbide, which is known as the active catalyst for heavy hydrocarbon formation in FTS[96], and to enhance the chemisorption and dissociation of CO_2[123]. Also, by cycling reactants, CO_2 conversion is increased. Therefore, finding suitable multifunctional catalyst combinations or promoters and optimizing the reactors should be an attractive area of research in the future. Dual-promoter systems are usually designed to improve the RWGS reaction activity, while increasing FTS activity and C_{5+} selectivity. Finally, there is a significant gap between the quality of synthesized liquid fuels and commercial gasoline. The octane number would be enhanced by developing catalysts that increase the fraction of isoparaffins in the gasoline.

Finally, the challenges to produce higher alcohols are considered. For higher alcohols synthesis, the major obstacles are the formation and insertion of the hydroxyl group during the C–C coupling process in the presence of parallel reactions. This is made even more challenging since the formation pathways are different over Fe- and Co-based catalysts and the mechanisms are controversial. On K/Fe/N-functionalized CNT catalysts, alcohol synthesis was explained by the reaction between hydrocarbon species, such as alkylidenes (R-CH_2-CH =), and *OH, which forms from the dissociation of adsorbed CO (*CO) and H_2 (*H)[73]. *CO was hypothesized to react with *CH_3 species to form *CH_3CO, which was then hydrogenated to form CH_3CH_2OH on a Na-Co/SiO_2 catalyst. To increase the yield of higher alcohols, efficient Co-based catalysts with more stable cobalt carbide (Co-Co_2C) interfaces and/or Co-M alloy nanocrystals should be developed. Co_2C is responsible for CO adsorption on the surface, whereas the Co metal is useful for CO dissociation and subsequent carbon-chain growth[124]. The synthesis of higher alcohols requires precise coordination between C–C coupling and OH formation, otherwise, more methanol or long-chain hydrocarbons would be produced. Also, the synergy of high metal dispersion and a high-density of hydroxyl groups on the supports can promote the selectivity to ethanol because the hydroxyls are able to stabilize formate species and protonate methanol[18]. The work from Fan's group also indicates that metal oxyhydroxides, such as FeOOH[125], $TiO(OH)_2$[1], and $ZrO(OH)_2$[126] can accelerate the CO_2 sorption and desorption processes, thus reducing the energy required for CO_2 capture based on experimental and DFT calculations. These metal oxyhydroxides are likely catalyst candidates because they

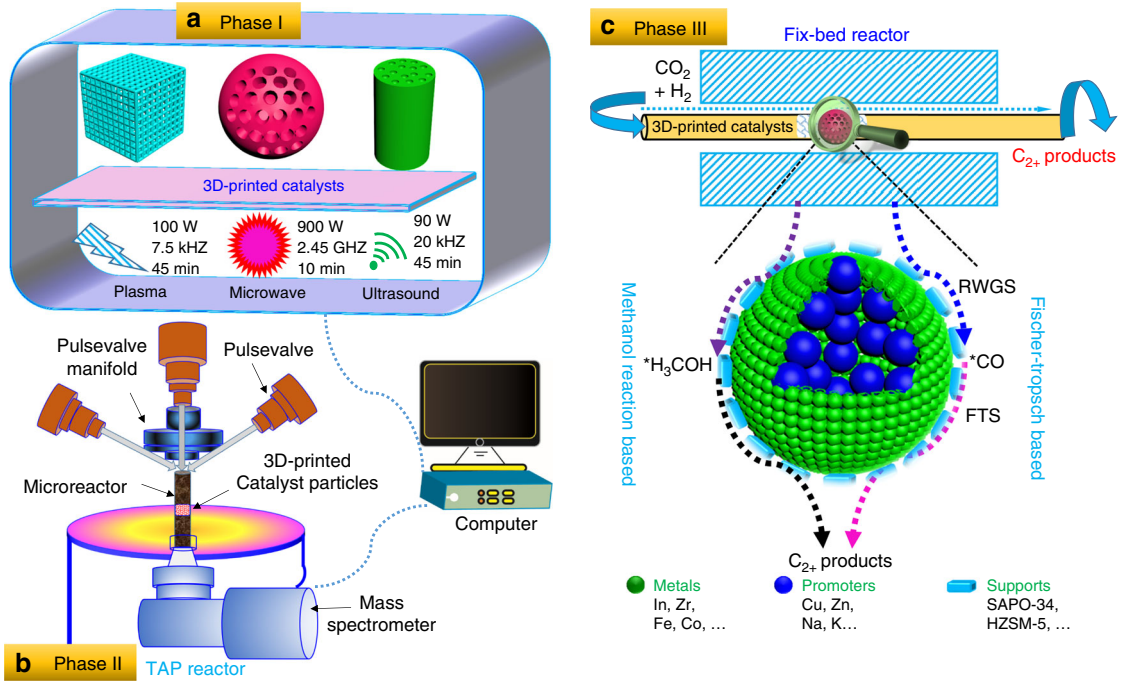

Fig. 5 Scheme of AI-guided development of CO_2 hydrogenation catalysts. Phase I is to prepare and modify catalysts using 3D printing technologies and new material modification technologies, such as plasma, microwave, and ultrasound modification[135,137,138]. Phase II is to use advanced techniques to characterize the catalysts. Phase III is to perform AI-guided evaluation of the catalysts.

contain hydroxyl groups that should enhance CO_2 hydrogenation to higher alcohols.

Transformational technologies for catalyst development. Revolutionary material manufacturing, characterization, and evaluation technologies emerging in the new century may be instrumental for hydrogenating CO_2 to high-value products. However, these technologies are only beginning to be explored for their application to CO_2 hydrogenation. Thus, this perspective endeavors to fill in critical blanks. The keys are to discover alternative catalysts, modify current catalysts for CO_2 activation, develop methods to prepare specialized catalysts on a large-scale, and intelligently evaluate catalysts. Guided by reaction theories and the associated heterogeneous catalytic CO_2 hydrogenation experimental results, the feasibility of transformational technologies in three phases of CO_2 hydrogenation will be explored: catalyst preparation and modification, characterization, and AI-guided evaluation (see Fig. 5).

Phase I is CO_2 hydrogenation catalyst preparation and modification. Conventional labor-intensive lab-based CO_2 hydrogenation catalyst preparation may be replaced by low-cost 3D-printing approaches to include characteristics of high mechanical strength and surface-to-volume ratio, with precise control of porosity, size, and shape[127]. The development of 3D-printed catalysts with designable and tunable structures is appealing and potentially useful for catalyst synthesis on a large scale. Although green 3D-printing has been utilized in preparing highly active, reusable, and stable catalysts for CO_2 removal, methane combustion, methanol to olefins conversion, syngas methanation, and N-aryl compound synthesis[128–131], it has not been used for CO_2 hydrogenation or CO_2 conversion catalysts to date. Also, most of the printed catalysts are millimeter- to micrometer-sized materials, while nano- or atomic-sized catalysts are still challenging to print by existing 3D printing technology. As the functional components of active CO_2 hydrogenation catalysts are further studied (e.g., metals, promoters, and supports), more effort can be devoted to incorporating them into a fully integrated platform with diverse microstructures by 3D printing. As different spatial arrangements in bifunctional catalysts influence catalytic performance, 3D printing can assemble the components with multiple structures in their preferred configuration. Therefore, 3D printing provides an alternative approach for preparation of novel CO_2 hydrogenation catalysts, especially for synthesizing bifunctional catalysts. Realizing that AI has proven to be a great tool in a range of fields, including materials discovery and design[132], the authors intend to apply a pioneering outlook with its application to CO_2 hydrogenation catalyst preparation, especially in combination with 3D printing technology. The 3D printing strategy already has advantages in potential scale-up manufacturing of catalysts, and AI technology would accelerate its application. AI-assisted 3D printing technologies can open new possibilities for the large-scale conversion of CO_2.

Also, new material modification technologies, such as microwave, ultrasound, and plasma treatments, have been suggested to modify catalysts for CO_2 activation, especially if the particle sizes or metal dispersion are affected by the 3D printing technologies. The utilization of unconventional modification tools in catalyst preparation and treatment can improve active phase dispersion to obtain a more uniform morphology with smaller particle sizes compared to the untreated catalysts[133–135]. Smaller particle size would enhance specific surface area and the exposed active sites available. The catalyst mechanical strength and the average basic site strength for CO_2 adsorption can be increased by microwave irradiation treatment, due to its better heat transfer[133]. Catalysts synthesized with the assistance of ultrasound, microwave, or plasma treatments have been employed in CO_2 hydrogenation and CO_2/CH_4 reforming reactions[134,136]. These unconventional methods need high frequency and input power with reduced processing time[135,137,138]. In addition, the reactor can be constructed with plasma or microwave enhancement. The CO_2-to-CH_3OH reaction was accomplished in a plasma reactor without heating or adding pressure, generating a CH_3OH selectivity of 53.7% and a CO_2 conversion of 21.2% over a Cu/γ-Al_2O_3 catalyst[136]. Coupling of plasma and catalyst lowered the kinetic barrier and energy cost associated with conventional high temperature and high pressure processing. Therefore, the use of these new modification technologies before or after 3D printing can possibly remedy defects introduced by 3D printing technologies.

Phase II is to characterize the CO_2 hydrogenation catalysts. New material characterization technologies, including in situ scanning transmission electron microscopy and temporal analysis of product reactors, coupled with qualitative and/or quantitative species identification, such as gas chromatography–mass spectrometry, are suggested for characterization of the catalysts prepared with state-of-the-art and transformational technologies. To date, in situ CO_2-temperature programmed surface reaction and diffuse reflectance infrared Fourier transform spectroscopy have been applied widely to elucidate how CO_2 molecules dynamically interact with the catalyst. However, other characterization methods for heterogeneous catalysts under in situ conditions are challenging due to the lack of experimental facilities. Therefore, in the future, AI-assisted CO_2 hydrogenation catalyst characterizations are needed. Machine learning especially can bring advanced computational techniques to the forefront of characterization of heterogeneous catalysts. For example, machine learning can be used to help interpret experimental spectra. Although the imaging and spectroscopic results are complicated, it would be helpful to design new catalysts and link models and experiments by connecting these results to structure–function information[139]. Timoshenko et al.[140] have successfully deciphered the 3D geometric structure of supported Pt NPs with the use of X-ray absorption near-edge structure (XANES) spectroscopy and supervised machine learning. They solved the structures and reconstructed the morphology of Pt NPs just from the experimental XANES data using an artificial neural network. Therefore, theoretical simulations can assist in obtaining more spectra and deconvoluting the structural characterization.

Phase III is to perform AI-guided evaluation of CO_2 hydrogenation catalysts. The prospect of using AI for identification of reaction intermediates and pathways and establishing kinetic models would be promising. First, the AI-guided method is expected to predict catalytic performance and to discover promising catalyst candidates. AI-based catalyst evaluation might largely help predict and improve catalyst stability, which however will require more significant effort. Zahrt et al.[141] pointed out that machine learning has the potential to change the way chemists select and optimize catalysts. Some examples of recent results in AI-based catalyst evaluation follow. The hydrocarbon selectivities for DME conversion can be accurately predicted by an AI model with an R^2 greater than 0.98 compared to experimental results[142]. Several known and unknown electrocatalysts for CO_2 reduction and hydrogen evolution were identified from 1499 intermetallics by machine learning[27]. Specifically, 258 candidate surfaces among 102 alloys have been identified from 23,141 adsorption sites for the H_2 evolution reaction.

Currently, it is inconvenient to characterize catalyst structures in situ during stability tests. Thus, in situ monitoring of the catalyst structure dynamics and transformation by AI would be beneficial. Second, we need more automatic, integrated, and flexible set-ups to evaluate catalysts. Third, data analysis could be

performed and kinetic models evaluated with the help of AI. Numerous experimental data for CO_2 hydrogenation have been generated and this existing data should be reanalyzed. Kitchin suggests that machine learning can be applied to build models with more sophisticated methods[143], generating new relevant data and calculated properties. Furthermore, it is crucial to identify reaction intermediates and pathways by AI. A simple syngas reaction on Rh(111) exhibits more than 2000 potential pathways[144], in comparison with the more complicated CO_2 hydrogenation reaction routes that are strongly influenced by the various active centers. Hence, it is necessary to analyze the reaction mechanism by employing machine learning and DFT calculations.

Finally, predicting relationships among the characteristics of the catalysts, such as Lewis acidity, CO_2 conversion efficiency, and product selectivity, with AI based on the available experimental data and DFT computation results will be helpful for discussing structure–function relationships and accelerating the discovery of catalytic mechanisms. Although AI offers many promising applications in CO_2 hydrogenation, robust and versatile AI is still in a primitive stage. A difficulty for AI development comes from the slowly developing applications of big data and a convenient language or software. Li et al.[28] pointed out that it is crucial and challenging to build additional criteria for screening and synthesizing catalysts, to quantify the uncertainties of machine-learning models, and to develop fingerprints of more sophisticated active sites with targeted functionalities. Also, more data for machine learning are required, including all reactions related to CO_2, such as FTS, CO_2/CH_4 reforming, and CO_2 hydrogenation. In conclusion, the collaborative efforts from experts and scientists in catalysis and materials design, machine-learning practitioners, and algorithm developers all over the world are needed to promote its development.

Received: 28 March 2019; Accepted: 18 November 2019;
Published online: 13 December 2019

References

1. Lai, Q. et al. Catalyst-TiO(OH)$_2$ could drastically reduce the energy consumption of CO_2 capture. *Nat. Commun.* **9**, 2672 (2018). ***This paper introduces a robust nanostructured TiO(OH)$_2$ catalyst for CO_2 capture at low temperature.***
2. Cui, S. et al. Mesoporous amine-modified SiO_2 aerogel: a potential CO_2 sorbent. *Energ. Environ. Sci.* **4**, 2070–2074 (2011).
3. Richard, A. R. & Fan, M. Low-pressure hydrogenation of CO_2 to CH_3OH using Ni-In-Al/SiO_2 catalyst synthesized via a phyllosilicate precursor. *ACS Catal.* **7**, 5679–5692 (2017).
4. Rogelj, J. et al. Paris agreement climate proposals need a boost to keep warming well below 2 °C. *Nature* **534**, 631–639 (2016).
5. Davis, S. J., Caldeira, K. & Matthews, H. D. Future CO_2 emissions and climate change from existing energy infrastructure. *Science* **329**, 1330–1333 (2010).
6. Jin, F. et al. High-yield reduction of carbon dioxide into formic acid by zero-valent metal/metal oxideredox cycles. *Energ. Environ. Sci.* **4**, 881–884 (2011).
7. Sun, Y. et al. In situ hydrogenation of CO_2 by Al/Fe and Zn/Cu alloy catalysts under mild conditions. *Chem. Eng. Technol.* **42**, 1223–1231 (2019).
8. Lyu, L., Zeng, X., Yun, J., Wei, F. & Jin, F. No catalyst addition and highly efficient dissociation of H_2O for the reduction of CO_2 to formic acid with Mn. *Environ. Sci. Technol.* **48**, 6003–6009 (2014).
9. Zhong, H. et al. Selective conversion of carbon dioxide into methane with a 98% yield on an in situ formed Ni nanoparticle catalyst in water. *Chem. Eng. J.* **357**, 421–427 (2019).
10. Yang, Y. et al. Synergetic conversion of microalgae and CO_2 into value-added chemicals under hydrothermal conditions. *Green Chem.* **21**, 1247–1252 (2019).
11. Wang, Y. et al. Exploring the ternary interactions in Cu-ZnO-ZrO_2 catalysts for efficient CO_2 hydrogenation to methanol. *Nat. Commun.* **10**, 1166 (2019).
12. Yan, Y., Dai, Y. H., He, H., Yu, Y. B. & Yang, Y. H. A novel W-doped Ni-Mg mixed oxide catalyst for CO_2 methanation. *Appl. Catal. B Environ.* **196**, 108–116 (2016).
13. Kothandaraman, J., Goeppert, A., Czaun, M., Olah, G. A. & Prakash, G. K. Conversion of CO_2 from air into methanol using a polyamine and a homogeneous ruthenium catalyst. *J. Am. Chem. Soc.* **138**, 778–781 (2016).
14. Roy, S., Cherevotan, A. & Peter, S. C. Thermochemical CO_2 hydrogenation to single carbon products: Scientific and technological challenges. *ACS Energy Lett.* **3**, 1938–1966 (2018).
15. Saravanan, K., Ham, H., Tsubaki, N. & Bae, J. W. Recent progress for direct synthesis of dimethyl ether from syngas on the heterogeneous bifunctional hybrid catalysts. *Appl. Catal. B Environ.* **217**, 494–522 (2017).
16. Li, Z. et al. Highly selective conversion of carbon dioxide to lower olefins. *ACS Catal.* **7**, 8544–8548 (2017).
17. Wei, J. et al. Directly converting CO_2 into a gasoline fuel. *Nat. Commun.* **8**, 15174–15181 (2017). ***This paper reports a multifunctional catalyst with three types of active sites for CO_2 hydrogenation to gasoline fuel.***
18. Yang, C. et al. Hydroxyl-mediated ethanol selectivity of CO_2 hydrogenation. *Chem. Sci.* **10**, 3161–3167 (2019). ***This paper highlights the synergism of high metal dispersion and high-density hydroxyl groups in promoting the selectivity to ethanol.***
19. Wu, J., Huang, Y., Ye, W. & Li, Y. CO_2 reduction: from the electrochemical to photochemical approach. *Adv. Sci.* **4**, 1700194 (2017).
20. Prieto, G. Carbon dioxide hydrogenation into higher hydrocarbons and oxygenates: thermodynamic and kinetic bounds and progress with heterogeneousand homogeneous catalysis. *ChemSusChem* **10**, 1056–1070 (2017).
21. Wang, W., Wang, S., Ma, X. & Gong, J. Recent advances in catalytic hydrogenation of carbon dioxide. *Chem. Soc. Rev.* **40**, 3703–3727 (2011).
22. Alvarez, A. et al. Challenges in the greener production of formates/formic acid, methanol, and DME by heterogeneously catalyzed CO_2 hydrogenation processes. *Chem. Rev.* **117**, 9804–9838 (2017).
23. Olah, G. A., Mathew, T. & Prakash, G. K. Chemical formation of methanol and hydrocarbon ("Organic") derivatives from CO_2 and H_2-carbon sources for subsequent biological cell evolution and life's origin. *J. Am. Chem. Soc.* **139**, 566–570 (2017).
24. Jia, J. et al. Heterogeneous catalytic hydrogenation of CO_2 by metal oxides: defect engineering-perfecting imperfection. *Chem. Soc. Rev.* **46**, 4631–4644 (2017).
25. Kattel, S., Liu, P. & Chen, J. G. Turning selectivity of CO_2 hydrogenation reactions at the metal/oxide interface. *J. Am. Chem. Soc.* **139**, 9739–9754 (2017).
26. Gao, P. et al. Direct conversion of CO_2 into liquid fuels with high selectivity over a bifunctional catalyst. *Nat. Chem.* **9**, 1019–1024 (2017). ***This paper reports discovery of an In_2O_3/HZSM-5 bifunctional catalyst for CO_2 hydrogenation to C_{5+} hydrocarbons through methanol intermediates.***
27. Tran, K. & Ulissi, Z. W. Active learning across intermetallics to guide discovery of electrocatalysts for CO_2 reduction and H_2 evolution. *Nat. Catal.* **1**, 696–703 (2018).
28. Li, Z., Wang, S. & Xin, H. Toward artificial intelligence in catalysis. *Nat. Catal.* **1**, 641–642 (2018). ***This paper points out the development and challenges of the implementation of artificial intelligence in catalysis.***
29. Parra-Cabrera, C., Achille, C., Kuhn, S. & Ameloot, R. 3D printing in chemical engineering and catalytic technology: structured catalysts, mixers and reactors. *Chem. Soc. Rev.* **47**, 209–230 (2018).
30. Samson, K. et al. Influence of ZrO_2 structure and copper electronic state on activity of Cu/ZrO_2 catalysts in methanol synthesis from CO_2. *ACS Catal.* **4**, 3730–3741 (2014).
31. Rui, N. et al. CO2 hydrogenation to methanol over Pd/In_2O_3: effects of Pd and oxygen vacancy. *Appl. Catal. B Environ.* **218**, 488–497 (2017).
32. Kattel, S., Ramírez, P. J., Chen, J. G., Rodriguez, J. A. & Liu, P. Active sites for CO_2 hydrogenation to methanol on Cu/ZnO catalysts. *Science* **355**, 1296–1299 (2017). ***This paper studies model catalysts and identifies a synergy of Cu and ZnO at the interface to form methanol through formate intermediates.***
33. Behrens, M. et al. The active site of methanol synthesis over Cu/ZnO/Al_2O_3 industrial catalysts. *Science* **336**, 893–897 (2012).
34. Bansode, A. & Urakawa, A. Towards full one-pass conversion of carbon dioxide to methanol and methanol-derived products. *J. Catal.* **309**, 66–70 (2014).
35. Rungtaweevoranit, B. et al. Copper nanocrystals encapsulated in Zr-based metal-organic frameworks for highly selective CO_2 hydrogenation to methanol. *Nano Lett.* **16**, 7645–7649 (2016).
36. An, B. et al. Confinement of ultrasmall Cu/ZnO_x nanoparticles in metal-organic frameworks for selective methanol synthesis from catalytic hydrogenation of CO_2. *J. Am. Chem. Soc.* **139**, 3834–3840 (2017).
37. Lam, E. et al. Isolated Zr surface sites on silica promote hydrogenation of CO_2 to CH_3OH in supported Cu catalysts. *J. Am. Chem. Soc.* **140**, 10530–10535 (2018).

38. Larmier, K. et al. CO_2-to-methanol hydrogenation on Zirconia-supported copper nanoparticles: Reaction intermediates and the role of the metal-support interface. *Angew. Chem. Int. Ed.* **56**, 2318–2323 (2017).
39. Sun, K. H. et al. Hydrogenation of CO_2 to methanol over In_2O_3 catalyst. *J. CO_2 Util.* **12**, 1–6 (2015).
40. Martin, O. et al. Indium oxide as a superior catalyst for methanol synthesis by CO_2 hydrogenation. *Angew. Chem. Int. Ed.* **55**, 6261–6265 (2016).
41. Li, H. et al. Synergetic interaction between neighbouring platinum monomers in CO_2 hydrogenation. *Nat. Nanotechnol.* **13**, 411–417 (2018).
42. Nie, X. et al. Mechanistic understanding of alloy effect and water promotion for Pd-Cu bimetallic catalysts in CO_2 hydrogenation to methanol. *ACS Catal.* **8**, 4873–4892 (2018).
43. Yin, Y. et al. Pd@zeolitic imidazolate framework-8 derived PdZn alloy catalysts for efficient hydrogenation of CO_2 to methanol. *Appl. Catal. B Environ.* **234**, 143–152 (2018).
44. Studt, F. et al. Discovery of a Ni-Ga catalyst for carbon dioxide reduction to methanol. *Nat. Chem.* **6**, 320–324 (2014).
45. Fiordaliso, E. M. et al. Intermetallic $GaPd_2$ nanoparticles on SiO_2 for low-pressure CO_2 hydrogenation to methanol: catalytic performance and in situ characterization. *ACS Catal.* **5**, 5827–5836 (2015).
46. Yang, X. et al. Low pressure CO_2 hydrogenation to methanol over gold nanoparticles activated on a CeO_x/TiO_2 interface. *J. Am. Chem. Soc.* **137**, 10104–10107 (2015).
47. Toyao, T., Kayamori, S., Maeno, Z., Siddiki, S. M. A. H. & Shimizu, K.-i Heterogeneous Pt and MoOx Co-loaded TiO_2 catalysts for low-temperature CO_2 hydrogenation to form CH_3OH. *ACS Catal.* **9**, 8187–8196 (2019).
48. Richard, A. R. & Fan, M. The effect of lanthanide promoters on NiInAl/SiO_2 catalyst for methanol synthesis. *Fuel* **222**, 513–522 (2018).
49. Ham, H., Baek, S. W., Shin, C.-H. & Bae, J. W. Roles of structural promoters for direct CO_2 hydrogenation to dimethyl ether over ordered mesoporous bifunctional Cu/M–Al_2O_3 (M = Ga or Zn). *ACS Catal.* **9**, 679–690 (2018).
50. Yang, G., Tsubaki, N., Shamoto, J., Yoneyama, Y. & Zhang, Y. Confinement effect and synergistic function of H-ZSM-5/Cu-ZnO-Al_2O_3 capsule catalyst for one-step controlled synthesis. *J. Am. Chem. Soc.* **132**, 8129–8136 (2010).
51. Phienluphon, R. et al. Designing core (Cu/ZnO/Al_2O_3)–shell (SAPO-11) zeolite capsule catalyst with a facile physical way for dimethyl ether direct synthesis from syngas. *Chem. Eng. J.* **270**, 605–611 (2015).
52. Dang, S. et al. Role of zirconium in direct CO_2 hydrogenation to lower olefins on oxide/zeolite bifunctional catalysts. *J. Catal.* **364**, 382–393 (2018).
53. Gao, J., Jia, C. & Liu, B. Direct and selective hydrogenation of CO_2 to ethylene and propene by bifunctional catalysts. *Catal. Sci. Technol.* **7**, 5602–5607 (2017).
54. Gao, P. et al. Direct production of lower olefins from CO_2 conversion via bifunctional catalysis. *ACS Catal.* **8**, 571–578 (2018).
55. Liu, X. et al. Selective transformation of carbon dioxide into lower olefins with a bifunctional catalyst composed of $ZnGa_2O_4$ and SAPO-34. *Chem. Commun.* **54**, 140–143 (2018).
56. Chen, J. et al. Hydrogenation of CO_2 to light olefins on CuZnZr@(Zn-)SAPO-34 catalysts: Strategy for product distribution. *Fuel* **239**, 44–52 (2019).
57. Ni, Y. et al. Selective conversion of CO_2 and H_2 into aromatics. *Nat. Commun.* **9**, 3457 (2018).
58. Jiao, F. et al. Selective conversion of syngas to light olefins. *Science* **351**, 1065–1068 (2016). ***This paper presents an OX-ZEO catalyst with high selectivity towards light olefins that breaks through the limitation of the ASF model.***
59. Liu, X. et al. Effective and highly selective CO generation from CO_2 using a polycrystalline α-Mo_2C catalyst. *ACS Catal.* **7**, 4323–4335 (2017).
60. Posada-Perez, S. et al. Highly activeAu/δ-MoC and Cu/δ-MoC catalysts for the conversion of CO_2: The metal/C ratio as a key factor defining activity, selectivity, and stability. *J. Am. Chem. Soc.* **138**, 8269–8278 (2016).
61. Ma, Z. & Porosoff, M. D. Development of tandem catalysts for CO_2 hydrogenation to olefins. *ACS Catal.* **9**, 2639–2656 (2019).
62. Zhao, B., Liu, Y., Zhu, Z., Guo, H. & Ma, X. Highly selective conversion of CO_2 into ethanol on Cu/ZnO/Al_2O_3 catalyst with the assistance of plasma. *J. CO_2 Util.* **24**, 34–39 (2018).
63. Kattel, S. et al. CO_2 hydrogenation over oxide-supported PtCo catalysts: the role of the oxide support in determining the product selectivity. *Angew. Chem. Int. Ed.* **55**, 7968–7973 (2016).
64. Tsoukalou, A. et al. Structural evolution and dynamics of an In_2O_3 Catalyst for CO_2 hydrogenation to methanol: an operando XAS-XRD and in situ TEM study. *J. Am. Chem. Soc.* **141**, 13497–13505 (2019). ***This paper displays the activation, stable performance, and deactivation of an In_2O_3 catalyst for methanol synthesis by an operando examination.***
65. Liu, L. et al. Mechanistic study of Pd–Cu bimetallic catalysts for methanol synthesis from CO_2 hydrogenation. *J. Phys. Chem. C* **121**, 26287–26299 (2017).
66. Ye, J., Liu, C., Mei, D. & Ge, Q. Active oxygen vacancy site for methanol synthesis from CO_2 hydrogenation on In2O3(110): a DFT study. *ACS Catal.* **3**, 1296–1306 (2013).
67. Tang, Q., Shen, Z., Russell, C. K. & Fan, M. Thermodynamic and kinetic study on carbon dioxide hydrogenation to methanol over a Ga_3Ni_5(111) surface: the effects of step edge. *J. Phys. Chem. C* **122**, 315–330 (2018).
68. Martínez-Suárez, L., Siemer, N., Frenzel, J. & Marx, D. Reaction network of methanol synthesis over Cu/ZnO nanocatalysts. *ACS Catal.* **5**, 4201–4218 (2015).
69. Olsbye, U. et al. Conversion of methanol to hydrocarbons: how zeolite cavity and pore size controls product selectivity. *Angew. Chem. Int. Ed.* **51**, 5810–5831 (2012).
70. Shi, J., Wang, Y., Yang, W., Tang, Y. & Xie, Z. Recent advances of pore system construction in zeolite-catalyzed chemical industry processes. *Chem. Soc. Rev.* **44**, 8877–8903 (2015).
71. Li, Z. et al. Highly selective conversion of carbon dioxide to aromatics over tandem catalysts. *Joule* **3**, 1–14 (2019). ***This paper reports stable catalysts that achieve high selectivity towards aromatics and demonstrate the effect of H_2O and CO_2 in promoting aromatics formation.***
72. Numpilai, T., Wattanakit, C., Chareonpanich, M., Limtrakul, J. & Witoon, T. Optimization of synthesis condition for CO_2 hydrogenation to light olefins over In_2O_3 admixed with SAPO-34. *Energy Convers. Manag.* **180**, 511–523 (2019).
73. Kangvansura, P. et al. Product distribution of CO_2 hydrogenation by K- and Mn-promoted Fe catalysts supported on N -functionalized carbon nanotubes. *Catal. Today* **275**, 59–65 (2016).
74. Chew, L. M. et al. Effect of nitrogen doping on the reducibility, activity and selectivity of carbon nanotube-supported iron catalysts applied in CO_2 hydrogenation. *Appl. Catal. A Gen.* **482**, 163–170 (2014).
75. Kattel, S., Liu, P. & Chen, J. G. Tuning selectivity of CO_2 hydrogenation reactions at the metal/oxide interface. *J. Am. Chem. Soc.* **139**, 9739–9754 (2017).
76. Zhang, J. et al. Promotion effects of Ce added Fe–Zr–K on CO_2 hydrogenation to light olefins. *React. Kinet. Mech. Cat.* **124**, 575–585 (2018).
77. Numpilai, T. et al. Structure–activity relationships of Fe-Co/K-Al_2O_3 catalysts calcined at different temperatures for CO_2 hydrogenation to light olefins. *Appl. Catal. A Gen.* **547**, 219–229 (2017).
78. Wang, X. et al. Effect of preparation methods on the structure and catalytic performance of Fe–Zn/K catalysts for CO 2 hydrogenation to light olefins. *Chin. J. Chem. Eng.* **26**, 761–767 (2018).
79. Ishida, T. et al. Synthesis of higher alcohols by Fischer–Tropsch synthesis over alkali metal-modified cobalt catalysts. *Appl. Catal. A Gen.* **458**, 145–154 (2013).
80. Galvis, H. M. T. et al. Supported iron nanoparticles as catalysts for sustainable production of lower olefins. *Science* **335**, 835–838 (2012).
81. Visconti, C. G. et al. CO_2 hydrogenation to lower olefins on a high surface area K-promoted bulk Fe-catalyst. *Appl. Catal. B Environ.* **200**, 530–542 (2017).
82. Meiri, N. et al. Novel process and catalytic materials for converting CO_2 and H_2 containing mixtures to liquid fuels and chemicals. *Faraday Discuss.* **183**, 197–215 (2015).
83. Ramirez, A., Gevers, L., Bavykina, A., Ould-Chikh, S. & Gascon, J. Metal organic framework-derived iron catalysts for the direct hydrogenation of CO_2 to short chain olefins. *ACS Catal.* **8**, 9174–9182 (2018). ***This paper illustrates K promotion effects in CO_2 hydrogenation and the importance of MOF-derived heterogeneous catalysts.***
84. Martinelli, M. et al. CO_2 reactivity on Fe–Zn–Cu–KFischer–Tropsch synthesis catalysts with different K-loadings. *Catal. Today* **228**, 77–88 (2014).
85. Wang, W., Jiang, X., Wang, X. & Song, C. Fe–Cu bimetallic catalysts for selective CO_2 hydrogenation to olefin-rich C_2^+ hydrocarbons. *Ind. Eng. Chem. Res.* **57**, 4535–4542 (2018).
86. Wang, J., You, Z., Zhang, Q., Deng, W. & Wang, Y. Synthesis of lower olefins by hydrogenation of carbon dioxide over supported iron catalysts. *Catal. Today* **215**, 186–193 (2013).
87. Mattia, D. et al. Towards carbon-neutral CO_2 conversion to hydrocarbons. *ChemSusChem* **8**, 4064–4072 (2015).
88. Gupta, S., Jain, V. K. & Jagadeesan, D. Fine tuning the composition and nanostructure of Fe-Based core-shell nanocatalyst for efficient CO_2 hydrogenation. *ChemNanoMat* **2**, 989–996 (2016).
89. Wu, T. et al. Porous graphene-confined Fe-K as highly efficient catalyst for CO_2 direct hydrogenation to light olefins. *ACS Appl. Mater. Inter.* **10**, 23439–23443 (2018).
90. Ding, J. et al. CO_2 hydrogenation to light olefins with high-performance $Fe_{0.30}Co_{0.15}Zr_{0.45}K_{0.10}O_{1.63}$. *J. Catal.* **377**, 224–232 (2019). ***This paper reveals that both oxygen vacancies and surface hydroxyl groups play significant roles in adsorption and activation of CO_2.***
91. Jiang, F., Liu, B., Geng, S., Xu, Y. & Liu, X. Hydrogenation of CO_2 into hydrocarbons: enhanced catalytic activity over Fe-based Fischer–Tropsch catalysts. *Catal. Sci. Technol.* **8**, 4097–4107 (2018).
92. Wei, J. et al. Catalytic hydrogenation of CO_2 to isoparaffins over Fe-based multifunctional catalysts. *ACS Catal.* **8**, 9958–9967 (2018). ***This paper reports***

a one-step high-yield synthesis of isoparaffins using Na-Fe$_3$ O$_4$ /HMCM-22 catalyst through CO$_2$ modified Fischer-Tropsch mechanism.
93. Cui, X. et al. Selective production of aromatics directly from carbon dioxide hydrogenation. *ACS Catal.* **9**, 3866–3876 (2019).
94. Tarasov, A. L., Isaeva, V. I., Tkachenko, O. P., Chernyshev, V. V. & Kustov, L. M. Conversion of CO_2 into liquid hydrocarbons in the presence of a Co-containing catalyst based on the microporous metal-organic framework MIL-53(Al). *Fuel Process. Technol.* **176**, 101–106 (2018).
95. Isaeva, V. I. et al. Fischer-Tropsch synthesis over MOF-supported cobalt catalysts (Co@MIL-53(Al). *Dalton Trans.* **45**, 12006–12014 (2016).
96. Shi, Z. et al. Effect of alkali metals on the performance of CoCu/TiO_2 catalysts for CO_2 hydrogenation to long-chain hydrocarbons. *Chin. J. Catal.* **39**, 1294–1302 (2018).
97. He, Z. et al. Synthesis of liquid fuel via direct hydrogenation of CO_2. *Proc. Natl Acad. Sci. USA* **116**, 12654–12659 (2019).
98. He, Z. et al. Water-enhanced synthesis of higher alcohols from CO_2 hydrogenation over a Pt/Co_3O_4 catalyst under milder conditions. *Angew. Chem. Int. Ed.* **55**, 737–741 (2016).
99. Li, S. et al. Effect of iron promoter on structure and performance of K/Cu–Zn catalyst for higher alcohols synthesis from CO_2 hydrogenation. *Catal. Lett.* **143**, 345–355 (2013).
100. Wang, L. et al. Selective hydrogenation of CO_2 to ethanol over cobalt catalysts. *Angew. Chem. Int. Ed.* **57**, 6104–6108 (2018).
101. Ko, J., Kim, B.-K. & Han, J. W. Density functional theory study for catalytic activation and dissociation of CO_2 on bimetallic alloy surfaces. *J. Phys. Chem. C* **120**, 3438–3447 (2016).
102. Willauer, H. D. et al. Modeling and kinetic analysis of CO_2 hydrogenation using a Mn and K-promoted Fe catalyst in a fixed-bed reactor. *J. CO_2 Util.* **3-4**, 56–64 (2013).
103. Nakhaei Pour, A., Housaindokht, M. R. & Monhemi, H. A new LHHW kinetic model for CO_2 hydrogenation over an iron catalyst. *Prog. React. Kinet. Mec.* **41**, 159–169 (2016).
104. Gunasooriya, G. T. K. K., van Bavel, A. P., Kuipers, H. P. C. E. & Saeys, M. Key role of surface hydroxyl groups in C–O activation during Fischer–Tropsch synthesis. *ACS Catal.* **6**, 3660–3664 (2016).
105. Owen, R. E., Mattia, D., Plucinski, P. & Jones, M. D. Kinetics of CO_2 hydrogenation to hydrocarbons over Iron-Silica catalysts. *ChemPhysChem* **18**, 3211–3218 (2017).
106. Riedel, T. et al. Fischer-Tropsch on iron with H_2/CO and H_2/CO_2 as synthesis gases: the episodes of formation of the Fischer-Tropsch regime and construction of the catalyst. *Top. Catal.* **26**, 41–54 (2003).
107. Su, T. et al. Density functional theory study on the interaction of CO_2 with Fe_3O_4 (111) surface. *Appl. Surf. Sci.* **378**, 270–276 (2016).
108. Nie, X. et al. Mechanistic insight into C–C coupling over Fe–Cu bimetallic catalysts in CO_2 hydrogenation. *J. Phys. Chem. C* **121**, 13164–13174 (2017).
109. Nie, X. et al. DFT insight into the effect of potassium on the adsorption, activation and dissociation of CO_2 over Fe-based catalysts. *Phys. Chem. Chem. Phys.* **20**, 14694–14707 (2018).
110. Bonura, G. et al. Catalytic behaviour of a bifunctional system for the one step synthesis of DME by CO_2 hydrogenation. *Catal. Today* **228**, 51–57 (2014).
111. Frusteri, F. et al. Stepwise tuning of metal-oxide and acid sites of CuZnZr-MFI hybrid catalysts for the direct DME synthesis by CO_2 hydrogenation. *Appl. Catal. B Environ.* **176-177**, 522–531 (2015).
112. Fujiwara, M., Satake, T., Shiokawa, K. & Sakurai, H. CO_2 hydrogenation for C_{2+} hydrocarbon synthesis over composite catalyst using surface modified HB zeolite. *Appl. Catal. B Environ.* **179**, 37–43 (2015).
113. Graça, I. et al. CO_2 hydrogenation into CH_4 on NiHNaUSY zeolites. *Appl. Catal. B Environ.* **147**, 101–110 (2014).
114. Olsbye, U. Single-pass catalytic conversion of syngas into olefins via methanol. *Angew. Chem. Int. Ed.* **55**, 7294–7295 (2016).
115. Boreriboon, N., Jiang, X., Song, C. & Prasassarakich, P. Fe-based bimetallic catalysts supported on TiO_2 for selective CO_2 hydrogenation to hydrocarbons. *J. CO_2 Util.* **25**, 330–337 (2018).
116. Choi, Y. H. et al. Sodium-containing spinel zinc ferrite as a catalyst precursor for the selective synthesis of liquid hydrocarbon fuels. *ChemSusChem* **10**, 4764–4770 (2017).
117. Yue, H. et al. A copper-phyllosilicate core-sheath nanoreactor for carbon-oxygen hydrogenolysis reactions. *Nat. Commun.* **4**, 2339–2346 (2013).
118. Gao, Y., Liu, S., Zhao, Z., Tao, H. & Sun, Z. Heterogeneous catalysis of CO_2 hydrogenation to C_{2+} products. *Acta Phys. Chim. Sin.* **34**, 858–872 (2018).
119. Liu, J. et al. Direct transformation of carbon dioxide to value-added hydrocarbons by physical mixtures of Fe_5C_2 and K-Modified Al_2O_3. *Ind. Eng. Chem. Res.* **57**, 9120–9126 (2018).
120. Liu, J. et al. Pyrolyzing ZIF-8 to N-doped porous carbon facilitated by iron and potassium for CO_2 hydrogenation to value-added hydrocarbons. *J. CO_2 Util.* **25**, 120–127 (2018).
121. Liu, J. et al. Fe-MOF-derived highly active catalysts for carbon dioxide hydrogenation to valuable hydrocarbons. *J. CO_2 Util.* **21**, 100–107 (2017).
122. Geng, S., Jiang, F., Xu, Y. & Liu, X. Iron-based Fischer-Tropsch synthesis for the efficient conversion of carbon dioxide into isoparaffins. *ChemCatChem* **8**, 1303–1307 (2016).
123. Choi, Y. H. et al. Carbon dioxide Fischer-Tropsch synthesis: a new path to carbon-neutral fuels. *Appl. Catal. B Environ.* **202**, 605–610 (2017).
124. Pei, Y. P. et al. High alcohols synthesis via Fischer-Tropsch reaction at cobalt metal/carbide interface. *ACS Catal.* **5**, 3620–3624 (2015).
125. Dutcher, B. et al. Use of nanoporous FeOOH as a catalytic support for $NaHCO_3$ decomposition aimed at reduction of energy requirement of Na_2CO_3/$NaHCO_3$ based CO_2 separation technology. *J. Phys. Chem. C* **115**, 15532–15544 (2011).
126. Wu, Y. et al. First-principles and experimental studies of $[ZrO(OH)]^{1+}$ or $ZrO(OH)_2$ for enhancing CO_2 desorption kinetics – imperative for significant reduction of CO_2 capture energy consumption. *J. Mater. Chem. A* **6**, 17671–17681 (2018).
127. Ruiz-Morales, J. C. et al. Three dimensional printing of components and functional devices for energy and environmental applications. *Energ. Environ. Sci.* **10**, 846–859 (2017). ***This paper reviews the progress and future prospects of 3D printing for energy and environmental applications***.
128. Tubío, C. R. et al. 3D printing of a heterogeneous copper-based catalyst. *J. Catal.* **334**, 110–115 (2016).
129. Li, Y. H. et al. Rational design and preparation of hierarchical monoliths through 3D printing for syngas methanation. *J. Mater. Chem. A* **6**, 5695–5702 (2018).
130. Michorczyk, P., Hedrzak, E. & Wegrzyniak, A. Preparation of monolithic catalysts using 3D printed templates for oxidative coupling of methane. *J. Mater. Chem. A* **4**, 18753–18756 (2016).
131. Thakkar, H. et al. 3D-printed zeolite monoliths for CO_2 removal from enclosed environments. *ACS Appl. Mater. Interfaces* **8**, 27753–27761 (2016).
132. Gómez-Bombarelli, R. Reaction: the near future of artificial intelligence in materials discovery. *Chemistry* **4**, 1189–1190 (2018).
133. Cai, W., de la Piscina, P. R., Toyir, J. & Homs, N. CO_2 hydrogenation to methanol over CuZnGa catalysts prepared using microwave-assisted methods. *Catal. Today* **242**, 193–199 (2015).
134. Asghari, S., Haghighi, M. & Taghavinezhad, P. Plasma-enhanced dispersion of Cr_2O_3 over ceria-doped MCM-41 nanostructured catalyst used in CO_2 oxidative dehydrogenation of ethane to ethylene. *Micropor. Mesopor. Mater.* **279**, 165–177 (2019).
135. Yahyavi, S. R., Haghighi, M., Shafiei, S., Abdollahifar, M. & Rahmani, F. Ultrasound-assisted synthesis and physicochemical characterization of Ni–Co/Al_2O_3–MgO nanocatalysts enhanced by different amounts of MgO used for CH_4/CO_2 reforming. *Energ. Convers. Manag.* **97**, 273–281 (2015).
136. Wang, L., Yi, Y., Guo, H. & Tu, X. Atmospheric pressure and room temperature synthesis of methanol through plasma-catalytic hydrogenation of CO_2. *ACS Catal.* **8**, 90–100 (2017).
137. Nayebzadeh, H., Haghighi, M., Saghatoleslami, N., Tabasizadeh, M. & Yousefi, S. Fabrication of carbonated alumina doped by calcium oxide via microwave combustion method used as nanocatalyst in biodiesel production: Influence of carbon source type. *Energ. Convers. Manag.* **171**, 566–575 (2018).
138. Khoja, A. H., Tahir, M. & Amin, N. A. S. Cold plasma dielectric barrier discharge reactor for dry reforming of methane over Ni/ɣ-Al_2O_3-MgO nanocomposite. *Fuel Process. Technol.* **178**, 166–179 (2018).
139. Goldsmith, B. R., Esterhuizen, J., Liu, J.-X., Bartel, C. J. & Sutton, C. Machine learning for heterogeneous catalyst design and discovery. *AIChE J.* **64**, 2311–2323 (2018).
140. Timoshenko, J., Lu, D., Lin, Y. & Frenkel, A. I. Supervised machine-learning-based determination of three-dimensional structure of metallic nanoparticles. *J. Phys. Chem. Lett.* **8**, 5091–5098 (2017).
141. Zahrt, A. F. et al. Prediction of higher-selectivity catalysts by computer-driven workflow and machine learning. *Science* **363**, eaau5631 (2019). ***This paper reports a computationally guided workflow for chiral catalyst selection that is significant for asymmetric reaction development***.
142. Hajjar, Z., Khodadadi, A., Mortazavi, Y., Tayyebi, S. & Soltanali, S. Artificial intelligence modeling of DME conversion to gasoline and light olefins over modified nano ZSM-5 catalysts. *Fuel* **179**, 79–86 (2016).
143. Kitchin, J. R. Machine learning in catalysis. *Nat. Catal.* **1**, 230–232 (2018).
144. Ulissi, Z. W., Medford, A. J., Bligaard, T. & Norskov, J. K. To address surface reaction network complexity using scaling relations machine learning and DFT calculations. *Nat. Commun.* **8**, 14621 (2017).
145. Wang, P., Zha, F., Yao, L. & Chang, Y. Synthesis of light olefins from CO_2 hydrogenation over (CuO-ZnO)-kaolin/SAPO-34 molecular sieves. *Appl. Clay Sci.* **163**, 249–256 (2018).
146. Wang, Y. et al. Rationally designing bifunctional catalysts as an efficient strategy to boost CO_2 hydrogenation producing value-added aromatics. *ACS Catal.* **9**, 895–901 (2018).
147. Zhang, J. et al. Selective formation of light olefins from CO_2 hydrogenation over Fe–Zn–K catalysts. *J. CO_2 Util.* **12**, 95–100 (2015).
148. Sun, Y., Yang, G., Wen, C., Zhang, L. & Sun, Z. Artificial neural networks with response surface methodology for optimization of selective CO_2

hydrogenation using K-promoted iron catalyst in a microchannel reactor. *J. CO_2 Util.* **24**, 10–21 (2018).
149. Liu, S., Zhou, H., Song, Q. & Ma, Z. Synthesis of higher alcohols from CO_2 hydrogenation over Mo–Co–K sulfide-based catalysts. *J. Taiwan. Inst. Chem. Eng.* **76**, 18–26 (2017).
150. Bai, S. et al. Highly active and selective hydrogenation of CO_2 to ethanol by ordered Pd-Cu nanoparticles. *J. Am. Chem. Soc.* **139**, 6827–6830 (2017). ***This paper reports an ordered Pd_2 Cu/P25 catalyst for CO_2 hydrogenation to ethanol through boosting *CO hydrogenation to *HCO.***

Acknowledgements

This work was supported by the China Scholarship Council (File no. 201704910592), the "Strategic Priority Research Program" of the Chinese Academy of Sciences (XDA21020800), and University of Wyoming.

Author contributions

R.Y., J.D., and W.G. were responsible for preparing the whole paper; R.Y., J.D., W.G., and Q. L. contributed to the figure designing and drawing as well as comparisons of different types of reaction mechanisms; M.A. and C.R. contributed to the understanding of the intermediate formation and catalysis mechanisms involved in the paper; Q.Z., Y.W., Z.X., A. R. contributed to the understanding of the effects of catalyst structure on CO_2 conversion and product selectivity, M.F. and Y.Y. are the initiators, designers, and leaders of the work.

Competing interests

The authors declare no competing interests.

Additional information

Correspondence and requests for materials should be addressed to M.F. or Y.-G.Y.

Peer review information *Nature Communications* thanks the anonymous reviewers for their contribution to the peer review of this work.

Reprints and permission information is available at http://www.nature.com/reprints

Publisher's note Springer Nature remains neutral with regard to jurisdictional claims in published maps and institutional affiliations.